Trisk95 Downregulation to Enhance Mitochondrial Function for Improved Diabetic Wound Healing

By

Shumail Maqbool

(Registration No: 400874)

Department of Biomedicine

Atta-ur-Rehman School of Applied Biosciences

National University of Sciences & Technology (NUST)

Islamabad, Pakistan

(2024)

Trisk95 Downregulation to Enhance Mitochondrial Function for Improved Diabetic Wound Healing

By

Shumail Maqbool

(Registration No: 400874)

A thesis submitted to the National University of Sciences and Technology, Islamabad,

in partial fulfillment of the requirements for the degree of

Master of Science in
Molecular Medicine

Supervisor: Dr. Hussain Mustatab Wahedi

Atta-ur-Rehman School of Applied Biosciences

National University of Sciences & Technology (NUST)

Islamabad, Pakistan

(2024)

THESIS ACCEPTANCE CERTIFICATE

Certified that final copy of MS Thesis written by Mr / Ms Shumail Maqbool (Registration No. 400874), of ASAB, NUST (School/College/Institute) has been vetted by undersigned, found complete in all respects as per NUST Statutes/ Regulations/ Masters Policy, is free of plagiarism, errors, and mistakes and is accepted as partial fulfillment for award of Masters degree. It is further certified that necessary amendments as point out by GEC members and evaluators of the scholar have also been incorporated in the said thesis.

Signature: Dr. Hussain Mustatab Wahedi, Associate Professor, Dept. of Biomedicine, ASAB - NUST, H-12, Islamabad

Name of Supervisor Dr. Hussain Mustatab Waheedi

Date: 23/09/24

Signature (HOD): Dr. Hussain Mustatab Wahedi, Head of Department (HoD), Dept. of Biomedicine, ASAB - NUST, H-12, Islamabad

Date: 23/09/24

Signature (Dean/ Principal) Prof. Dr. Muhammad Asghar, Principal & Dean, Atta-ur-Rahman School of Applied Biosciences (ASAB), NUST, Islamabad

Date: 24/09/24

FORM TH-4
(MUST BE TYPE WRITTEN)

National University of Sciences & Technology

MASTER THESIS WORK

We hereby recommend that the dissertation prepared under our supervision by: (Student Name & Regn No.) Shumail Maqbool 400874

Titled: **Trisk95 Downregulation to Enhance Mitochondrial Function for Improved Diabetic Wound Healing** be accepted in partial fulfillment of the requirements for the award of MS Molecular Medicine degree and awarded grade A Grade (Initial).

Examination Committee Members

1. Name: Dr. Muhammad Asghar Signature: Dr. Muhammad Asghar, Professor, Dept. of Biomedicine, ASAB - NUST, H-12, Islamabad

2. Name: Dr. Naila Naz Signature: Dr. Naila Naz, Professor, Dept. of Biomedicine, ASAB - NUST, H-12, Islamabad

3. Name: Dr. Muhammad Rizwan Alam Signature:

Supervisor's name: Dr Hussain Wahedi Signature: Dr. Hussain Mustatab Wahedi, Head of Department (HoD), Dept. of Biomedicine, ASAB - NUST, H-12, Islamabad

Date: 23/09/2024

Dr. Hussain Mustatab Wahedi, Head of Department (HoD), Dept. of Biomedicine, ASAB - NUST, H-12, Islamabad

Head of Department

24/09/24
Date

COUNTERSINGED

Date: 24/09/24

Dean/Principal

Prof. Dr. Muhammad Asghar
Principal & Dean
Atta-ur-Rahman School of Applied Biosciences (ASAB), NUST, Islamabad

AUTHOR'S DECLARATION

I **Shumail Maqbool** hereby state that my MS thesis titled "**Trisk95 downregulation to enhance mitochondrial function for improved diabetic wound healing**" is my own work and has not been submitted previously by me for taking any degree from National University of Sciences and Technology, Islamabad or anywhere else in the country/ world.

At any time if my statement is found to be incorrect even after I graduate, the university has the right to withdraw my MS degree.

Name of Student: Shumail Maqbool

Date: 24/09/2024

DEDICATION

This thesis is dedicated to the memory of my late ***Father****, whose enduring wisdom and love continue to guide me. To my* ***Mother*** *and* ***siblings, Awais Maqbool, Jawad Maqbool, Sidra Maqbool,*** *whose unwavering support and encouragement have provided the foundation for all my achievements, throughout my academic journey. This work is a tribute to the love, and support you have all provided****.***

ACKNOWLEDGEMENTS

I want to express my deepest gratitude to all those who have contributed to the completion of this thesis. I express my gratitude to the **Principal, Dr. Muhammad Asghar**, and **HoD, Dr. Hussain Mustatab Wahedi,** for their support.

I am profoundly grateful to my **supervisor, Dr. Hussain Mustatab Wahedi**, for his invaluable guidance, encouragement, and support throughout this research. Your insightful feedback and unwavering commitment to my academic growth have been instrumental in shaping the direction and quality of this work.

I also thank the members of my thesis committee, **Dr. Muhammad Asghar, Dr. Naila Naz**, and **Dr. Muhammad Rizwan Alam** for their thoughtful suggestions, constructive criticism, and support.

Finally, special thanks to **my family and friends**, **Aliya Jabeen,** who have always believed in me and provided constant motivation.

This thesis is the result of collective effort, and I am thankful to everyone who has contributed, directly or indirectly, to its completion.

TABLE OF CONTENTS

LIST OF TABLES

Page No.

LIST OF FIGURES

Page No.

LIST OF SYMBOLS, ABBREVIATIONS, AND ACRONYMS

BFT	Benfotiamine
IL-6	Interleukin-6
SOD	Superoxide dismutase
Cat	Catalase
ROS	Reactive Oxygen Species
ECM	Extracellular Matrix
DM	Diabetes Mellitus
TNF	Tumor Necrosis Factor
Ca^{2+}	Calcium
MCUC	Mitochondrial Calcium Uniporter Complex
RyR	Ryanodine Receptor
CSQ	Calsequestrin
SR	Sarcoplasmic Reticulum
GLUT	Glucose Transporters
HO^{-}	Hydroxyl Radicals
H_2O_2	Hydrogen Peroxide
ATP	Adenosine Triphosphate
NCLX	$Na^{+}/Ca^{2+}/Li^{+}$ Exchanger
MEMs	Mitochondrial Associated Membranes
UPR	Unfolded Protein Response
TPP	Thiamine Pyrophosphate
AGE	Advanced Glycation End Products
TK	Transketolase

NF-kB	Nuclear Factor-Kappa B
MAPK	Mitogen-Activated Protein Kinase
Pkb/Akt	Protein Kinase B
VEGF	Vascular Endothelial Growth Factor
PKC	Protein Kinase C
CMC	Carboxymethyl Cellulose
PTP	Permeability Transition Pore
TGF	Transforming Growth Factor
CRP	C-Reactive Protein
NOx	Nitrogen Oxides
EPCs	Endothelial Progenitor Cells

ABSTRACT

Impaired wound healing in diabetic patients is a major clinical challenge, often associated with mitochondrial dysfunction, increased inflammation, and oxidative stress. Trisk95, a transmembrane protein, plays a critical role in calcium homeostasis, and its modulation may enhance wound repair processes. Benfotiamine, a thiamine derivative, improves diabetic complications by affecting oxidative stress, inflammation, metabolism, and signaling pathways. This study aimed to evaluate the efficacy of benfotiamine in diabetic wound healing by impacting Trisk95 expression and exerting anti-inflammatory and antioxidant effects. Benfotiamine was administered topically to the wounded area of diabetic mice and the wound closure rate was measured. The anti-inflammatory effects were quantified by measuring interleukin-6 (IL-6) and interleukin-10 (IL-10) levels. Antioxidant effects were assessed by measuring reactive oxygen species (ROS) level, and the activity of superoxide dismutase (SOD) and catalase (Cat). Benfotiamine significantly downregulated Trisk95, IL-6, and ROS levels, and upregulated IL-10. It increased the activity of SOD and Cat enzymes. In conclusion, benfotiamine promotes wound healing in diabetic mice by modulating Trisk95 and exerting anti-inflammatory and antioxidant effects, thereby improving mitochondrial function.

Keywords: Trisk95, diabetic wound healing, mitochondrial function, antioxidant, anti-inflammatory

CHAPTER 1: INTRODUCTION

1.1 Skin

Skin is the largest organ of the body that acts as a protective barrier against solar radiations, pathogens, and fluid loss, and possesses neuro-immuno-endocrine functions, contributing to the maintenance of body homeostasis [2]. Functionally, the skin has two compartments: the epidermis, which includes keratinocytes, melanocytes, and Langerhans; and the dermis with fibroblasts, vasculature, and immune cells [3].

1.1.1 Skin Injury

In case of any injury to the skin, its integrity must be restored to maintain its function. Whenever acute skin damage occurs, skin wound regeneration protects against secondary infection and internal organ damage [4]. Rapid skin regeneration helps the body heal from injuries as a single organ, restores impaired bodily functioning, and lowers morbidity and death [5-7].

1.2 Wound Healing Phases

There are four phases of the biological skin repair process: hemostasis, which begins right after the injury and includes processes like platelet aggregation, vascular constriction, fibrin formation, and degranulation [8]. The second phase involves proper inflammation, where inflammatory cells, namely, neutrophils and monocytes, migrate to the wound site [9, 10]. The third is the proliferative phase which overlaps the inflammatory phase, characterized by re-epithelization, angiogenesis, and collagen and extracellular matrix (ECM) formation. Afterward, the remodeling phase takes place, involving collagen deposition and vascular maturation [11].

1.3 Wound Complexity

Wound repair is an intricate process, that is altered by various factors, affecting one or more phases. These factors include local factors i.e. ischemia, edema, infection, etc. as well as systemic factors like diabetes mellitus, hypothermia, sepsis, age, obesity, and medications [12].

1.4 Diabetes Mellitus

Diabetes mellitus (DM) is a critical health emergency of the 21st century [13]. This metabolic disorder is described as increased blood glucose levels because of inadequate production of insulin, insufficient use of insulin by body cells, or a combination of both factors [14]. In 2019, over 422 million individuals worldwide were reported to have diabetes and projections estimate a further rise to 578 million by 2030 [15]. Diabetes mellitus gives rise to various complications and the most common is impaired wound healing that frequently results in amputation [16, 17]. Of 25% of patients, 68% pass away within five years (Zhang, Li et al. 2023).

1.4.1 Diabetic Wound Healing

There is increased inflammatory cell infiltration and less granulation tissue formation in diabetic skin as compared to normal skin [19, 20]. Patients with diabetes mellitus have longer inflammatory phases during wound healing, accompanied by increased cytokines like interleukin (IL)-6, IL-1β, tumor necrosis factor-α (TNF-α) [21]. The increased infiltration of cytokines causes more damage to the tissue and impaired diabetic wound healing. In addition, hyperglycemia also leads to increased production of reactive oxygen species (ROS) which leads to oxidative injury [22, 23], due to a higher influx of reducing equivalents into the electron transport chain of mitochondria [24-26]. Increased oxidative stress and bacteria predisposed the wound to chronic wounds [27]. Therefore, prolonged inflammation is the major reason for impaired healing in diabetic wound patients, and alleviating the pro-inflammation and oxidative stress is crucial for accelerating the repair process in these patients [28].

In diabetic wounds, mitochondrial dysfunction is also observed [29]. The continuous elevation of blood glucose levels impairs mitochondrial function, increases ROS levels, and induces damage to mitochondrial DNA, thereby contributing to a delayed wound-healing process [30, 31].

1.5 Calcium (Ca^{2+}) Signaling

Elevation of intracellular Ca^{2+} in the wound-healing process is the first damage signal [32] that is crucial for initiating and regulating wound healing [33]. This Ca^{2+} propagation is accountable for different processes including modulation of fibroblast and keratinocyte

proliferation, migration, and differentiation during re-epithelialization [34, 35], and acts as an inflammatory mediator [36]. Additionally, it is involved in regulating angiogenesis in the wound-healing process [37] and the metabolism and formation of the extracellular matrix [38]. Ca^{2+} is also important in regulating mitochondrial function, activating action potential in the mitochondrial matrix to increase ATP production and other cofactors [39, 40]. Mitochondria regulate calcium uptake by mitochondrial calcium uniporter complex (MCUC) [41-44]. Increased calcium levels can affect mitochondrial function, altering mitochondrial metabolism and morphology [45-47]. Mitochondria exhibit specific phenotypes in response to high glucose levels in the skin, potentially attributed to calcium uptake which may lead to mitochondrial damage [1, 48].

1.6 Trisk95

Triadin, a transmembrane protein, is co-localized using the ryanodine receptor (RyR) on the junctional sarcoplasmic reticulum (SR) membrane. At first, it was identified as a 95-kDa protein [49-51]. Triadin interacts with various proteins including Junctin, Ryanodine receptor (RyR) [52, 53], and CSQ, contributing to the regulation of calcium homeostasis in cells [54]. Multiple isoforms of triadin are expressed in skeletal muscle [55]. One of these isoforms is the 95-kDa, named Trisk95 [56]. Trisk95 has a short cytoplasmic domain, a transmembrane domain, and a C-terminal domain residing within the lumen of the SR [57]. The intraluminal domain interacts with RyR and CSQ [58, 59]. It is present in skeletal and cardiac muscles and involved in the release of calcium from the sarcoplasmic reticulum, thus in muscles, it regulates excitation-contraction coupling [60]. Trisk95 binds directly to the RyR receptor and is involved in the controlled release of calcium from the SR by directly interacting with the RyR receptor [61].

1.6.1 Hyperglycemia and Trisk95

High blood glucose levels lead to more glucose uptake to the skin via the insulin-independent pathway. The mechanism by which skin takes up glucose is via Glut-1, its expression level increases with the increase in blood glucose level due to which glucose level increases in the diabetic mice skin than in healthy mice skin. This indicates that modification in the glucose concentration of blood regulates the glucose level in the skin. And increased skin glucose levels, lead to the upregulation of Trisk95 expression, evidencing that expression of Trisk95 is dependent on the glucose pathway [1].

1.6.2 Trisk95 and Calcium Homeostasis

Since in skeletal and cardiac muscles, Trisk95 is involved in the calcium release from the endoplasmic reticulum (ER) [41, 60], overexpression of Trisk95 caused by high glucose concentrations affects the amount of calcium in the ER store. RyR-1 and CSQ-2 are more highly expressed in diabetic mice and keratinocyte cell lines, cultured in high-glucose environments. In healthy people, Trisk95 does not bind to RyR-1 or CSQ-2, and RyR-1 channels sustain a continuous calcium outflow from the ER into the cytosol. However, in diabetic conditions, Trisk95 is upregulated. The RyR-1 channels close when the skin Trisk95/CSQ-2 complex binds to them and increases the calcium storage in the ER [1].

1.6.3 Trisk95 and Mitochondrial Dysfunction

Mitochondria regulate intracellular calcium, by the mitochondrial calcium uniporter complex (MCUC) activation [41, 42], impacting mitochondrial metabolism and network morphology [46, 47]. Increased ER calcium ultimately causes changes to the mitochondrial network, affecting its function. It triggers mitochondrial changes by increasing the MCU and MICU1 expression, activating the MCU complex in keratinocytes, and facilitating calcium uptake [1], causing mitochondrial damage [48].

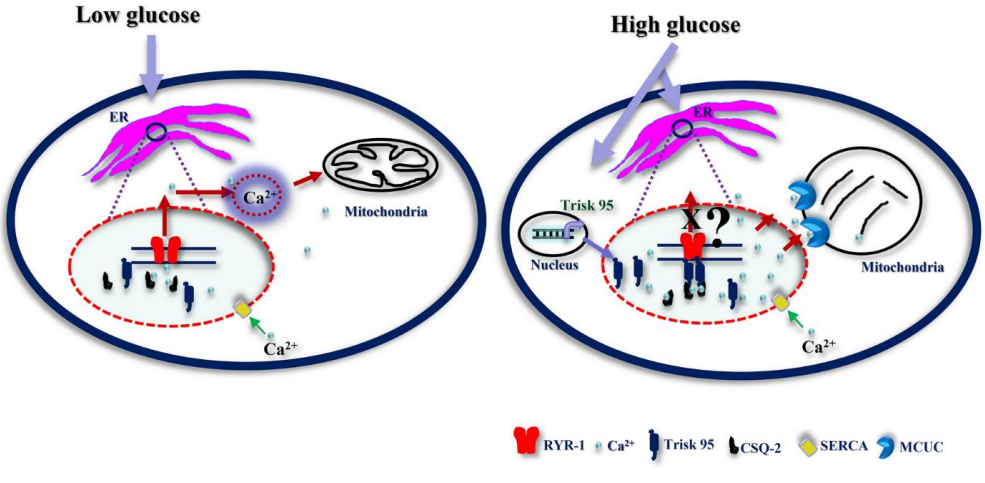

[1]

Figure 1.1: Hyperglycemia triggers calcium uptake in the ER and mitochondria by Trisk95

In mitochondria, Ca^{2+} homeostasis is important for cellular function and dysfunction. It regulates energy production, shapes intracellular Ca^{2+} signals, and influences cell death [62-64]. Ca^{2+} interacts with reactive oxygen species (ROS), for example, hydroxyl radicals (HO^{-}),

hydrogen peroxide (H_2O_2), and superoxide anion (O^{2-}), [65]. Ca^{2+} promotes ATP synthesis by stimulating mitochondrial enzymes, potentially leading to increased oxygen consumption and respiratory chain electron leakage, producing higher ROS levels [66].

1.7 Oxidative Stress

Oxidative stress is essential in the occurrence and development of diabetic wounds [19, 67]. It is referred to as insufficient antioxidant systems or oxidants and antioxidants imbalance, disrupting the redox signaling [68]. Oxygen-dependent, redox-sensitive signaling pathways play an essential role in the wound-healing process. Oxidative stress is crucial for wound cleaning, and it helps in wound repair, hemostasis, inflammation, angiogenesis, formation of tissue granulation, and extracellular matrix (ECM) formation and maturation [69, 70]. Excessive oxidative stress is, however, a major cause of diabetic wound healing [30]. Research revealed that the highly oxidizing environment is linked to tissue hypoxia and hyperglycemia that infiltrates diabetic wounds. People having long-term type 2 diabetes have markedly decreased levels of antioxidant enzyme activity [71], and higher ROS production, which damaged wound-healing processes by increasing apoptosis and senescence in cells with continuing lipid peroxidation, oxidative stress, DNA damage, and protein modification [69].

1.7.1 ROS and Inflammation

In addition, ROS is crucial in inflammatory diseases [72]. In dysregulated conditions, ROS is generated in reaction to any stimuli or defense mechanism that increases inflammation [73], and promotes inflammatory factor production by altering fibroblasts, endothelial cells, and keratinocytes [74-76]. This may result in inflammatory damage, cellular senescence, and cell death, impairing the healing process [77].

1.8 Inflammation

Inflammation is important for preparing for the initiation of wound repair [78-81]. One important step in preparing for starting wound healing is inflammation; the resolution of inflammation delay may give rise to a persistent and dysregulated response that exacerbates tissue damage [82]. In individuals with diabetes mellitus, the impairment of wound healing can be attributed to the emergence of chronic inflammation, which can be caused by proinflammatory macrophages losing their ability to change into anti-inflammatory ones [83].

Controlling microbial invasion requires the neutrophils' recruitment to the wound, but the persistence of neutrophils causes a delayed inflammatory phase resolution and delayed healing in diabetic wounds [84]. Chronic inflammation is caused by elevated and prolonged ROS generation in the wound. Hence, redox balance restoration improves inflammatory skin diseases [30].

1.8.1 Inflammation and ROS

Inflammatory mediators can enhance the generation of ROS within cells, increasing the resulting damage and disruption of metabolism [74]. Additionally, the respiratory bursts of inflammatory cells during inflammation result in increased ROS production and accumulation at the site of injury [85, 86].

1.9 Mitochondria

Mitochondria serve as the powerhouse of cells, playing a crucial role in energy production within the human body by respiratory chain and oxidative phosphorylation, and are involved in redox regulation, signal transduction, and cell death [87]. They are arranged in intricate intracellular networks connected to their physiological functions [88]. In response to environmental changes, mitochondria can rapidly and temporarily change their morphology, modifying their function involving Ca^{2+} homeostasis, redox signaling, metabolism, and energy production [89]. Mitochondria regulate cellular Ca^{2+} storage and propagation, as mitochondrial Ca^{2+} is crucial for several cellular signaling pathways and bioenergetics [90]. Ca^{2+} is introduced into the mitochondria via the mitochondrial Ca^{2+} uniporter complex (MCU) and is exported through the mitochondrial $Na^{+}/Ca^{2+}/Li^{+}$ exchanger (NCLX). However, due to the low affinity of mitochondria for Ca^{2+}, its transferal into the mitochondria mainly takes place through close interactions with the endoplasmic reticulum (ER), known as mitochondrial-associated membranes (MEMs) [91]. Various mitochondrial processes, including insulin signaling, glucose sensing, unfolded protein response (UPR), apoptosis, mitophagy, and ROS signaling, depend on these MEMs [47]. Mitochondria regulates the immune response. They act mainly as a central hub for metabolic regulation, which is required to activate multiple immune cell types of innate and acquired immunity. Mitochondria also participate in inflammatory signaling via ROS [92, 93], make scaffolds for cell-cell interactions between numerous immune cells and respective proteins [94], and directly trigger inflammatory responses [95].

1.9.1 Mitochondrial Dysfunction

Any abnormality in mitochondrial function can impact the healing process of diabetic wounds [96]. In diabetes, high glucose levels contribute to increased oxidative stress and ROS levels, leading to mitochondrial dysfunction [97]. This increased ROS level enhances mitochondrial permeability, increasing cytochrome c release and triggering cell apoptosis in diabetic wounds [98].

1.10 Benfotiamine

Benfotiamine (S-benzoyl thiamine-O-monophosphate) with higher bioavailability, is a synthetic S-acyl derivative of thiamine (vitamin B1). It is a lipid-soluble analog of thiamine and is almost completely insoluble in hydrophobic and organic solvents [99]. Benfotiamine undergoes dephosphorylation by membrane-bound S-benzoyl thiamine phosphatases. Intracellularly, thioesterases convert S-benzoyl thiamine into thiamine, a portion of which is phosphorylated by thiamine pyrophosphokinase into thiamine pyrophosphate (TPP), TPP serves as a coenzyme in glycolysis, the Krebs cycle, and the pentose phosphate pathway. Both thiamine and benfotiamine metabolites exhibit anti-inflammatory, antioxidative, and neuroprotective properties [100].

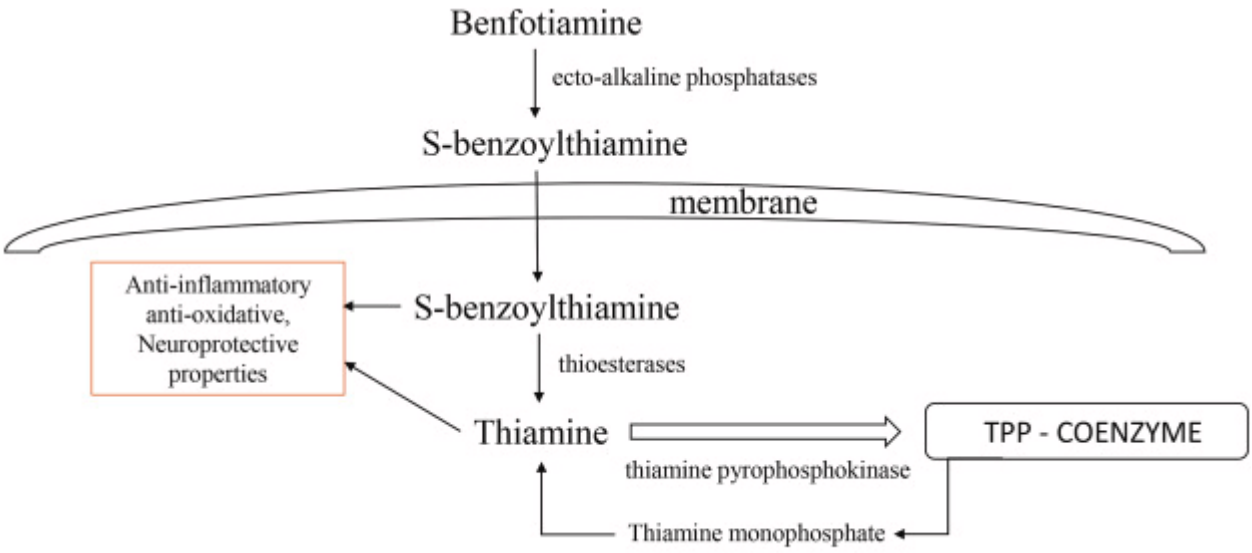

[100]

Figure 1.2: The metabolic pathways of benfotiamine

Benfotiamine is best known for its anti-inflammatory, anti-oxidative, and other therapeutic effects. It has been widely studied and used for treating diabetic complications, neurodegenerative diseases, and inflammatory conditions [100]. Notably, benfotiamine reduces superoxide production and also functions as a direct antioxidant [101].

Bozic et. al. show that benfotiamine suppresses oxidative stress, decreasing the production of nitric oxide, superoxide anion, and malondialdehyde. It also upregulates the antioxidant defense system by increasing the superoxide dismutase, catalase, and glutathione levels and activity. Thus benfotiamine is effective in alleviating both inflammation and oxidative stress [102].

As mentioned earlier, benfotiamine exhibits antioxidant properties that contribute to the amelioration of diabetic complications [101, 103]. In hyperglycaemic conditions, benfotiamine markedly enhances glucose oxidation and promotes the absorption of glucose [104].

Benfotiamine inhibits advanced glycation products (AGE) production thereby reducing metabolic stress. It can also modulate several signaling pathways including NF-kB, MAPK [105], PKB/Akt, VEGF [106], and transketolase pathways [107], affecting cell survival, repair, and cell death processes.

In high glucose levels, Benfotiamine regulates the intracellular glucose and counteracts the detrimental effects of hyperglycemia [108-111]. As in a high glucose environment, benfotiamine reduces the aldose reductase (AR) expression while increasing the transketolase (Tk) activity [112] and is associated with a decrease in protein kinase C (PKC) activation, protein glycation, and oxidative stress [113, 114].

Delayed diabetic wound healing is a worldwide issue that even leads to limb amputation. The large patient population and associated healthcare costs necessitate an effective treatment method. Diabetic wound development mechanisms are affected by multiple factors, including hyperglycemia, and impaired immune function. These mechanisms interact, leading to irreversible diabetic complications. Although current treatments, such as anti-infective treatment, advanced dressing application, and glycemic control aim to enhance wound healing, they often face limitations such as high costs, inconsistent results, and prolonged treatment periods. For this, benfotiamine is used to investigate its role in the healing process of diabetic wounds. It is an antioxidant that alleviates oxidative stress, and pro-inflammatory response and importantly mitigates hyperglycemia-induced stress complications. It was hypothesized that

benfotiamine would downregulate the Trisk95 that is related to hyperglycemia, induce mitochondrial dysfunction, and reduce oxidative stress and pro-inflammatory response thereby improving mitochondrial function by enhancing antioxidative and anti-inflammatory response, and regulating calcium homeostasis in the mitochondria by downregulating Trisk95, improving wound healing in diabetic mice.

OBJECTIVES

- To evaluate the potential of benfotiamine to downregulate Trisk95 in diabetic wound models
- To assess the effects of Trisk95 downregulation on ROS production
- To elucidate the antioxidant effect of benfotiamine in diabetic wound healing

CHAPTER 2: MATERIALS AND METHODS

2.1 Animal Experimentation

All the animal experiments were conducted per the ethical guidelines outlined in the NIH publication #85-23 (Revised 1985) on the Care and Use of Laboratory Animals.

2.2 Animal Model Strain

The experiments were conducted on Balb/c 6-7 weeks old male mice, (purchased from the National Institute of Health (NIH), Islamabad), weighing 25-35g. A proper humid and temperature-controlled room was provided to all the mice under standard conditions. All the mice were maintained in a 12-hour light-dark cycle, and free access to water and food was provided. The mice were placed in plastic cages, with approximately five per cage.

2.3 Diabetes Induction

The mice were acclimatized for 1 week before diabetes induction. To induce diabetes, mice were starved for 12 hours with free access to water. Following the fasting period, each mouse received a single intraperitoneal injection of Alloxan (200mg/kg in normal saline). After injection, the food was restored, and the mice were provided with a 20% sucrose solution for the next 12-18 hours to prevent hypoglycemic shock. After 12 hours, the sucrose solution was replaced with plain water. Diabetes was checked using a glucometer, and mice with blood glucose levels above 300mg/dl were considered diabetic.

2.4 Wound Creation

After the induction of diabetes, wounds were created in the mice. The mice were anesthetized using Ketamine (1mg/kg) injections. Hair removal cream was applied to the dorsal posterior region to remove excess hair, and the area was cleaned with ethanol. Then, a 6mm Biopsy Punch was used for the wound creation.

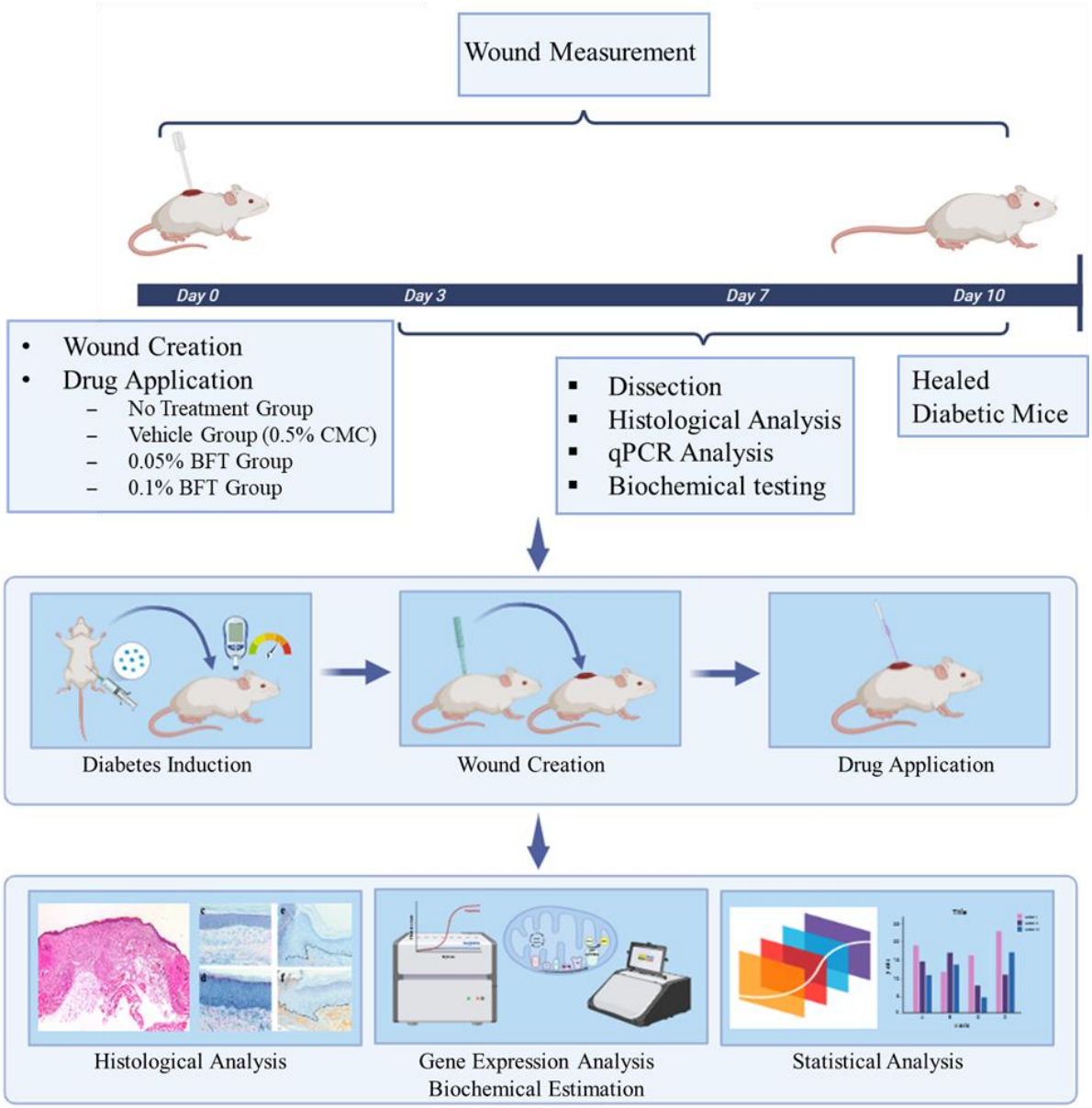

Figure 2. 1: Schematic diagram of overall experiment performed during the study

2.5 Drug Application

2.5.1 Animal Groups

The mice were randomly divided into four groups, each consisting of 7 mice (n=7):

Control Group: No treatment was given to this group.

Vehicle Group: 0.5% Carboxymethyl cellulose (CMC) was topically applied to this group.

BFT 0.05% Group: mice were treated topically with 0.05% benfotiamine.

BFT 0.1% Group: In this group, 0.1% benfotiamine was topically applied to the mice.

A 10-day experiment was performed and a daily 200uL solution of benfotiamine and CMC was applied topically on the wound by a dropper.

2.6 Wound Contraction Measurement

Pictures of the wound of each mouse were taken daily from day 1 to day 10 using a digital camera. A scale was included in each photograph to measure the wound size accurately. The specific wound area was analyzed statistically using ImageJ software. The healing rate was calculated using the following formulae for statistical analysis:

$$\text{Woundhealingrate}(\%) = \frac{A_0 - A_t}{A_0} \times 100\%$$

A_0 = initial wound areas on days 0

A_t = wound areas on days t

This formula gives a reduction in the wound area in percentage over time.

2.7 Tissue Collection

The specified number of mice were dissected on days 3, 7, and 10 of the protocol. The mice were euthanized using chloroform and quickly flayed with sharp scissors to extract the wounded area. The skin tissue was washed by ice-cold phosphate-buffered saline (PBS). After washing, the tissue samples were stored at -80°C until further analysis.

2.8 Histological Analysis

For histology, tissue samples of the wound were embedded in paraffin wax after being fixed in a 10% formalin solution. The 4μm-thick sections were cut and stained with hematoxylin and eosin (H&E), and Mason's trichrome per the standard method. Both stainings were analyzed and visualized under a light microscope.

2.9 Gene Expression Analysis

2.9.1 RNA Extraction

The tissue samples were weighed using a weighing balance. 500 µL Trizol was added in an Eppendorf tube for each 100 mg of tissue. The tissue was minced with scissors. After mincing for phase separation, chloroform was added, vortexed for 15 seconds and then the homogenate was incubated at room temperature for 5 minutes. The mixture was centrifuged at 14,000 rpm for 15 minutes at 4°C. The supernatant was separated using a micropipette and transferred to a different Eppendorf tube. For RNA precipitation, 150µL of isopropanol was added to the supernatant and 10 minutes of incubation was given to this sample on ice. The mixture was then centrifuged again at 14,000 rpm for 15 minutes at 4°C. After centrifugation, the supernatant was discarded, and the pellet was washed two times with 500µL of 70% ethanol. After washing, the pellet was vortexed with ethanol and centrifuged at 14,000 rpm for 15 minutes at 4°C. The supernatant was discarded, and the pellet was air-dried for 20-25 minutes. After drying, 25 µL of DEPC-treated water was added to the pellet and was vortexed for 30 seconds and stored at -80°C until further analysis.

2.9.2 RNA Quantification

After RNA extraction, RNA quantification was performed to assess the yield and purity of the isolated RNA, which was done using a NanoDrop spectrophotometer. The absorbance ratio was measured at 260 nm and 280 nm (A_{260}/A_{280}) to assess the purity of the RNA samples. Samples, exhibiting ratios between 1.8 and 2.0 were considered to contain minimal to no contamination, indicating high-quality RNA suitable for downstream applications. While the samples with ratios below 1.6 were considered significantly contaminated, and unsuitable for further experimentation.

2.9.3 cDNA Synthesis

The protocol followed for cDNA synthesis was according to the “Revert Aid First Strand cDNA synthesis kit” (Thermo Fisher, USA).

Table 2. 1: List of reagents for cDNA synthesis

Sr.#	**Reagents**	**Volume**
01	RNA Template	1-3 µg
02	Nuclease free water	8-10 µL
03	Random Hexamer primer	1 µL
04	10X PCR Buffer	4 µL
05	dNTP	2 µL
06	RNase Inhibitor	1 µL
07	Revert Aid RT	1 µL
	Total volume	20 µL

Reagents were completely thawed before starting the experiment. A 12 µL mixture was prepared, by adding the RNA template, nuclease-free water, and random hexamer primer in PCR tubes. The reaction mixture was then prepared by adding reagents in concentrations multiplied by the number of reactions, including the reaction buffer, dNTPs, RNase inhibitor, and Revert Aid Reverse Transcriptase. The PCR tubes were placed on ice, and all the reagents were added to get a final volume of 20 µL. The PCR tubes were placed in a PCR machine, and the conditions were set as outlined in Table 2.2. The synthesized cDNA was then stored at -20°C.

Table 2. 2: Thermocycler conditions for cDNA synthesis

Steps	**Temperature**	**Duration**
Annealing	25ºC	00:05:00
Incubation	42ºC	01:00:00
Reaction termination	85ºC	00:05:00

2.9.4 Confirmation of cDNA Synthesis

To confirm cDNA synthesis, conventional PCR was performed using GAPDH as the housekeeping gene.

Table 2. 3: Reagents for cDNA confirmation

Sr.#	**Reagents**	**Volume**
01	cDNA	1 µL
02	Taq buffer	2.5 µL
03	10mM dNTPs	0.5 µL
04	Nuclease Free water/dH_2O	17.3 µL
05	Forward Primer (specified)	1 µL
06	Reverse Primer (specified)	1 µL
07	Taq Polymerase	0.2 µL
08	$MgCl_2$	1.5 µL
	Total Volume	25 µL

The reaction mixture was prepared by adding reagents in concentrations multiplied by the number of reactions, including Taq buffer, 10mM dNTPs, nuclease-free water, forward and reverse primers, Taq polymerase, and $MgCl_2$. Subsequently, 24 µL of the reaction mixture was added to each PCR tube with 1 µL of cDNA, making the final volume 25 µL. The PCR tubes were then placed in a PCR machine and subjected to the reaction conditions specified in Table 2.4.

Table 2. 4: conventional PCR reaction conditions

Stages	**Temperature**	**Duration**
Initial denaturation	95°C	00:03:00
Denaturation	95°C	00:00:30
Annealing	60°C	00:00:30
Extension	72°C	00:00:45
Final extension	72°C	00:05:00
Final hold	4°C	Till further processing

2.9.5 Primer Designing

Primers were designed using the qPCR analysis tool from Integrated DNA Technologies (IDT). The NM number of the desired gene was retrieved from the NCBI database and input into the IDT tool, which generated various primer sequences. A primer sequence meeting the desired criteria was selected, and further validation was performed using in-silico PCR and BLAT. After all validation steps, the final selected primer sequences are listed in Table 2.5.

Table 2. 5: Final primer sequences

Sr. #	**Gene**	**Primers**
01	Trisk95	Forward-GTTTTCCCAGAGGACCATGA Reverse-TTGGCAGCCAGCTAATCTTT
02	IL-6	Forward-TAGTCCTTCCTACCCCAATTTCC Reverse-TTGGTCCTTAGCCACTCCTTC
03	IL-10	Forward-GCTCTTACTGACTGGCATGAG Reverse-CGCAGCTCTAGGAGCATGTG
04	GAPDH	Forward-GCCTTCCGTGTTCCTACC Reverse-CCTCAGTGTAGCCCAAGATG

2.9.6 Primer Dilution/Reconstitution

The primers were received in lyophilized form. To prepare the stock solution, 50 µL of nuclease-free water was added to the lyophilized primers and incubated at -20°C. For primer dilutions, 5 µL of the stock primer solution was mixed with 45 µL of nuclease-free water to achieve a 10µM solution.

2.9.7 Primer Optimization

For primer optimization, conventional PCR was performed, and the products were analyzed by gel electrophoresis to visualize the bands for each primer. The reagents used in the PCR setup are listed in Table 2.6. The PCR tubes were then placed in the PCR machine, and the reaction conditions were set according to those specified in Table 2.7.

Table 2. 6: Reagents for primer optimization

Sr. No.	**Reagents**	**Volume**
01	cDNA	1 µL
02	Taq buffer	2.5 µL
03	10Mm dNTPs	0.5 µL
04	Nuclease Free water/dH_2O	17.3 µL
05	Forward Primer (specified)	1 µL
06	Reverse Primer (specified)	1 µL
07	Taq Polymerase	0.2 µL
08	$MgCl_2$	1.5 µL
	Total Volume	25 µL

Table 2. 7: Reaction conditions for primer optimization

Stages	**Temperature**	**Duration**
Initial denaturation	95°C	00:03:00
Denaturation	95°C	00:00:30
Annealing	60°C	00:00:30
Extension	72°C	00:00:45
Final extension	72°C	00:05:00
Final hold	4°C	Till further processing

2.9.8 Agarose Gel Electrophoresis

For agarose gel electrophoresis, the first 10X TBE buffer was prepared with the reagents as in Table 2.8. All the reagents were added to the reagent bottle and add dH_2O to make the total volume 1000ml with pH-8.3. Then to make the 1X TBE buffer 1:9 dilution was made with 10X TBE buffer and dH_2O respectively.

A 2% agarose gel was prepared to observe the bands for primer optimization. To make the gel, 1 g of agarose (weighed using an electric balance) was dissolved in 50 mL of 1X TBE buffer in a conical flask and heated for 1 minute in a microwave oven until fully dissolved. After the temperature was dropped slightly, 6 µL of ethidium bromide was added and mixed thoroughly. The solution was then poured into a gel caster with a comb in place and left to solidify for 30 minutes. After solidification, the gel was carefully transferred to a horizontal gel tank filled with 1X TBE buffer. In a separate tube, 8 µL of PCR sample was mixed with 2 µL of 6X loading dye. Each sample was then loaded into the well of the gel using a micropipette, and the loading order was recorded carefully. The gel was then run at 90 volts for 40 minutes. After electrophoresis, the gel was carefully removed from the caster and transferred to the gel documentation system. The gel image was captured using the gel-Doc system.

Table 2. 8: Components of 10X TBE buffer

Sr#	Reagents	Quantity
01	Tris base	108g
02	Boric acid	55g
03	EDTA	40 mL
04	dH_2O	900ml

2.9.9 Quantitative real-time PCR (RT-PCR)

For the expression analysis of the target genes qPCR was performed. The reaction mixture was prepared with concentrations multiplied by the number of reactions, including forward and reverse primer, Eva green dye, and nuclease-free water. Then 9 µL of the reaction mixture was added to the PCR strips and 1 µL cDNA was added to each strip making the final volume 10 µL. The strips were then placed in the qPCR machine, and the reaction conditions were set according to Table 2.10. After completing the qPCR cycles, the Ct values were recorded to calculate the relative expression of the target gene. The housekeeping gene GAPDH was used as a control for each group, and each reaction was performed in triplicate.

Table 2. 9: Reagents of RT-PCR

Sr.#	Reagents	Volume
01	cDNA	1 µL
02	Forward primer	0.5 µL
03	Reverse primer	0.5 µL
04	Eva green dye	2 µL
05	Nuclease free water	6 µL
	Total volume	10 µL

Table 2. 10: Conditions for qPCR

Stages	**Temperature**	**Duration**	**Cycles**
Holding	95°C	00:10:00	01
Cycling			40
Step 1	95°C	00:00:15	
Step 2	60°C	00:00:30	
Step 3	72°C	00:00:30	
Melt curve			01
Step 1	95°C	00:00:10	
Step 2	60°C	00:01:00	
Step 3	97°C	00:00:05	

2.10 Biochemical Profiling

2.10.1 Protein Lysate

To make protein lysate of tissue samples RIPA buffer was prepared as in Table 2.11. then this RIPA buffer was added to the skin tissue samples according to the weight. Then the tissue was minced with scissors and incubated at room temperature for 10 minutes. After incubation the minced tissue was vortexed for 5 minutes and again incubated on ice for 10 minutes. After incubation, homogenized tissue was centrifuged at 14000rpm, 4°C, for 10 minutes. After centrifugation, the supernatant was separated in another Eppendorf and the pellet was discarded.

Table 2. 11: RIPA buffer reagents

Sr#	Reagents	Quantity
01	10mM Tris-Cl/Base (pH-8.0)	0.0606g
02	1mM EDTA	0.0146g
03	140mM NaCl	0.4098
04	1% Triton X-100	0.5ml
05	0.1% SDS	0.05g
06	Sodium Deoxycholate	0.05g
	Total volume	49.5ml
07	Protease inhibitor	10µl/ml

2.10.2 Oxidative Stress Analysis

2.10.2.1 Reactive Oxygen Species (ROS) Measurement

For the ROS level measurement, reagent 1 (R1) (N, N-diethyl-para-phenylendiamine (DEPPD) in 0.1M sodium acetate buffer) and reagent 2 (R2) ($FeSO_4$ in 0.1M sodium acetate buffer) was prepared as in Table 2.12. Then R1 and R2 were mixed at a ratio of 1:25. Then 5µl sample and 140µl buffer were added to the 96 well plates and were incubated for 5 minutes at room temperature. After incubation 100µl R1:R2 was added in each well and the absorbance was recorded at 505nm using Agilent 8453 UV–Visible spectrophotometer (UK). A buffer standard calibration curve was used for the measurement of ROS. The ROS levels were normalized with the total protein concentration.

Table 2. 12: Reagents for R1 and R2 preparation

Sr#	Reagents	Quantity
01	0.1M Sodium acetate buffer (pH-4.8)	50ml
02	DEPPD	100 µg/ml
03	$FeSO_4$	0.5%

2.10.3 Antioxidants Activity Measurement

2.10.3.1 Superoxide Dismutase (SOD)

For SOD measurements mixture was prepared as in Table 2.13. Then 5µl protein lysate was added to the 96-well plate and 243µl reaction mixture was in each well and was illuminated for 7 minutes with a fluorescence lamp. After this, it was incubated for 5 minutes at room temperature. After incubation 3µl chilled Riboflavin was added and then incubated for 8 minutes at room temperature. After incubation, 3 absorbance readings were recorded at 540nm with 1 minute difference.

Table 2. 13: Reagents for SOD reaction mixture preparation

Sr#	Reagents	Volume
01	9.9mM L-Methionine	1.5ml
02	57µM NBT	1ml
03	0.025% Triton X-100	0.75ml
04	50mM Potassium phosphate buffer	To make volume 30ml

2.10.3.2 Catalase

For catalase measurement 8.09 µl sample, 161µl 50mM potassium phosphate buffer pH-7, and 80.9µl 5.9mM H_2O_2 were added to the 96 well plate. The 3 absorbances were recorded at 240nm at 30-second intervals.

2.11 Statistical Analysis

Data was expressed as the mean ± standard deviation. The data was statistically analyzed using GraphPad Prism by one-way and two-way analysis of variance (ANOVA) followed by Tukey's test. The probability values of $p<0.05$ were considered statistically significant.

CHAPTER 3: RESULTS

3.1 Effect of Topical Application of Benfotiamine on Wound Closure in Diabetic Mice

The effect of the topical application of benfotiamine on wound healing in BALB/c wild-type diabetic mice was determined by comparing the four groups: No treatment (Control), Vehicle, 0.05% BFT, and 0.1% BFT. Wound sizes were analyzed for 10 days, with pictorial representation (Figure 3.1A), and quantitative measurements of wound healing (Figure 3.1B, C). Additionally, wound closure rates were calculated to evaluate the effectiveness of the treatment over time. To compare the wound area and closure rate among different treatment groups results were plotted in graphs. It was observed that wound size decreased in 0.1% of BFT-treated mice compared to the other groups (Figure 3.1A). On days 7 and 10, 0.1% of the BFT-treated group showed a significant reduction in wound size (12.5 and 9.4 mm^2 wound area with 61% and 71% closure rate respectively) compared to the other groups which did not contract significantly (Figure 3.1B). Even though there were no continuous significant variations in wound size, the 0.1% BFT group showed a higher overall wound closure rate and the fastest wound healing with a wound closure rate of 81% on the 10th day of treatment as compared to other groups (Figure 3.1C).

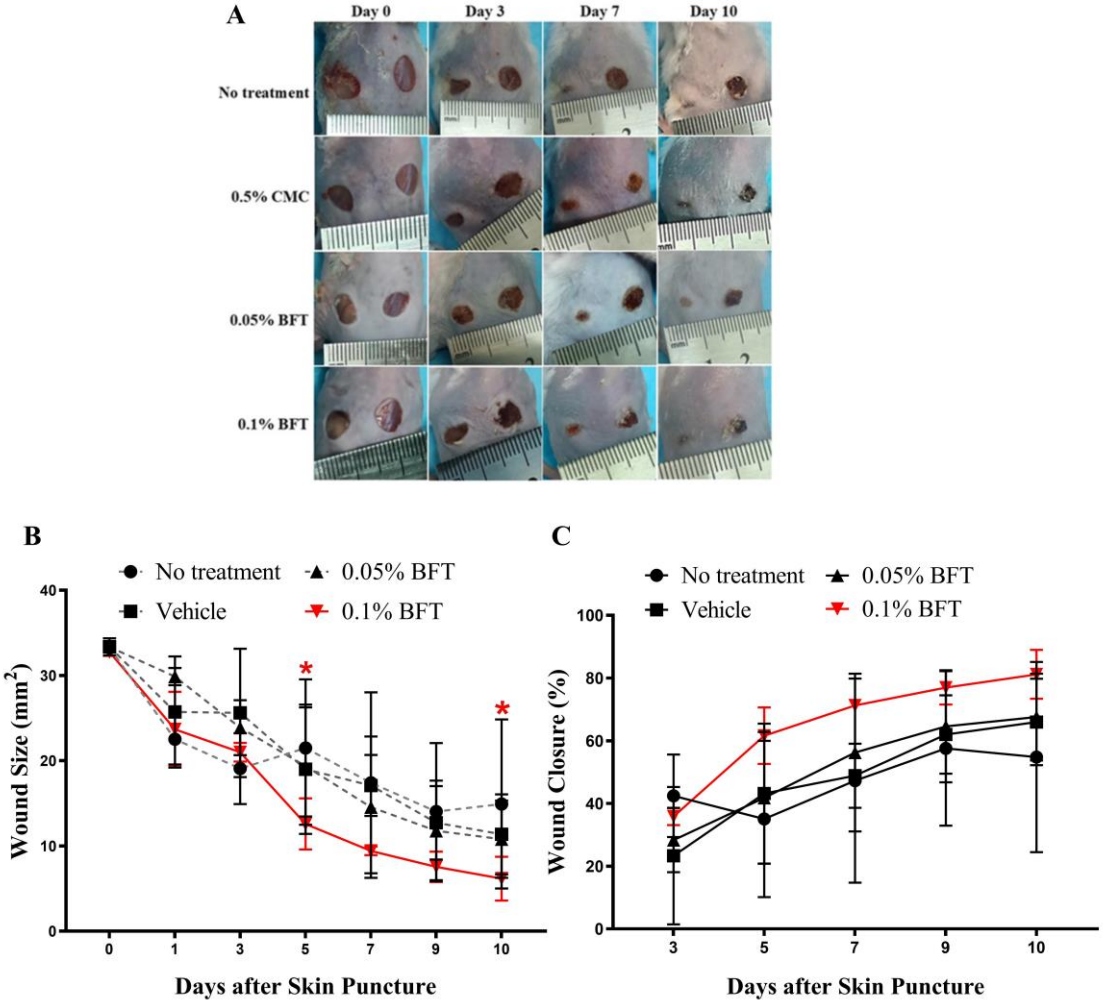

Figure 3. 1: Effect of benfotiamine on diabetic wound healing in BALB/c wild-type mice

(A) Photographic representation of wound healing processed on Days 0, 3, 7, and 10 after the puncture. (B) Graphical representation of average wound area on days 0, 1, 3, 5, 7, 9, 10 (n = 6). (C) Graphical representation of wound closure rate (%) on days 3, 5, 7, 9, 10 (n = 6). All the data was statistically analyzed by one-way ANOVA and is presented as mean ± SD. *$p < 0.05$ (0.1% BFT treatment group vs No treatment group).

3.2 Histological Analysis

3.2.1 Benfotiamine Promotes Epidermal Regeneration in Wounded Diabetic Mice

Then the benfotiamine effect on epidermal regeneration was evaluated in BALB/c wild-type diabetic mice in the four groups: No treatment (Control), Vehicle, 0.05% BFT, and 0.1% BFT on days 3, 7, and 10 by H&E staining. The staining data showed more epidermal regeneration in drug-treated groups on days 3, 7, and 10 (Figure 3.2A). Figure 3.2B also showed a significant increase in epidermal regeneration in benfotiamine-treated groups on days 3, 7, and 10.

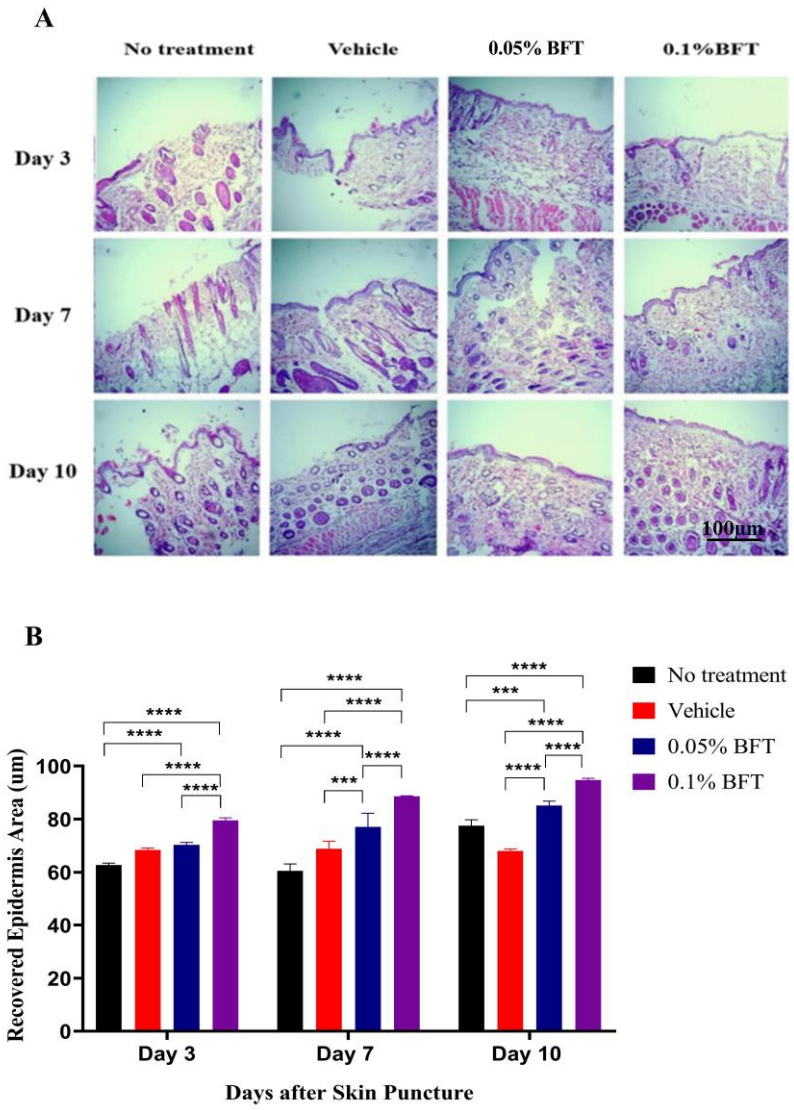

Figure 3. 2: Effect of benfotiamine on epidermal regeneration

(A) Epidermal regeneration was assessed through H&E staining on days 3, 7, and 10 of wounded skin samples of all groups. (B) Graphical representation of recovered epidermis area on Days 3, 7, and 10. All the data was statistically analyzed by one-way ANOVA and is presented as mean ± SD. ***$p < 0.001$, ****$p < 0.0001$ vs. no treatment and Vehicle group.

3.2.2 Benfotiamine Increases Collagen Deposition in Wounded Diabetic Mice

Then benfotiamine effect on collagen deposition was evaluated in BALB/c wild-type diabetic mice in the four groups: No treatment (Control), Vehicle, 0.05% BFT, and 0.1% BFT on days 3, 7, and 10 by Mason's trichrome staining. The staining data showed more collagen deposition in drug-treated groups on days 3, 7, and 10 (Figure 3.3A). Figure 3.3B also showed a significant increase in collagen deposition in benfotiamine-treated groups on days 3, 7, and 10.

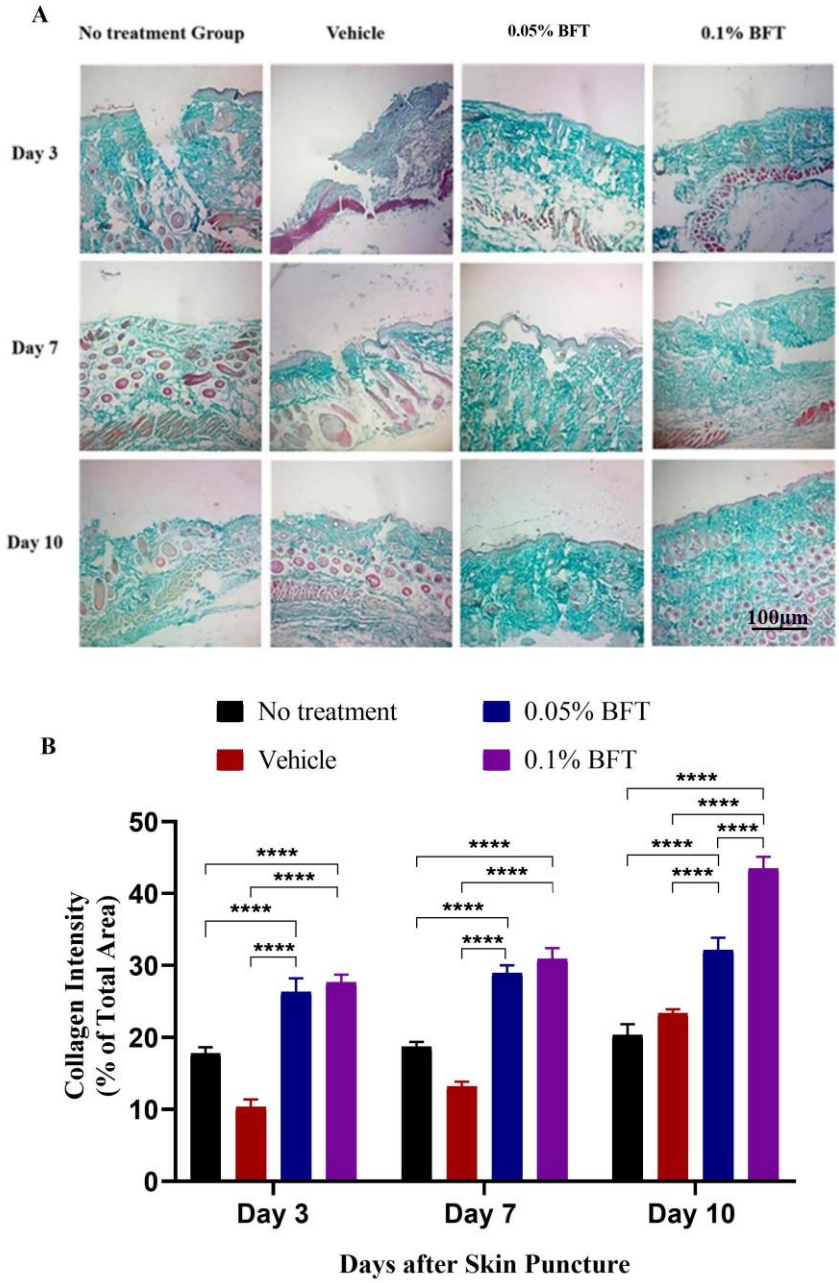

Figure 3. 3: Effect of benfotiamine on collagen deposition

(A) Collagen deposition was assessed through Masson's trichrome staining on days 3, 7, and 10 of wounded skin samples of all groups. (B) Graphical representation of collagen deposition on Days 3, 7, and 10. All the data was statistically analyzed by one-way ANOVA and is presented as mean ± SD. ****$p < 0.0001$ vs. no treatment and vehicle group.

3.3 mRNA Expression Analysis

3.3.1 Benfotiamine mitigates hyperglycemia-induced stress condition by downregulating Trisk95 Level

Then benfotiamine effect on Trisk95 was evaluated in BALB/c wild-type diabetic mice in the four groups: No treatment (Control), Vehicle, 0.05% BFT, and 0.1% BFT on days 3, 7, and 10. On day 3, it is shown that the Trisk95 level is consistent in all the groups. While on days 7 and 10, Trisk95 increased significantly in the vehicle group. On day 7, less increase in Trisk95 occurred in the 0.05% BFT group, and in the 0.1% BFT group, its level decreased significantly. On day 10, 0.1% BFT and 0.05% BFT groups showed significant downregulation of Trisk95 (Figure 3.4).

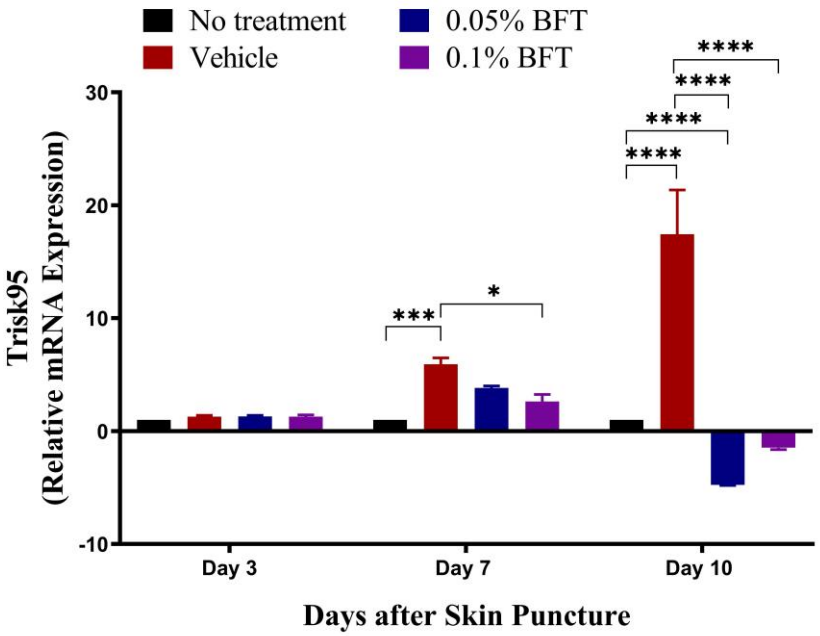

Figure 3. 4: Benfotiamine effect on Trisk95 level

Graphical representation of mRNA expression of Trisk95 on days 3, 7, and 10 of wounded skin samples of all groups. All the data was statistically analyzed by one-way ANOVA and is presented as mean ± SD. ****$p < 0.0001$, ***$p < 0.001$, *$p < 0.05$ vs No treatment group.

3.3.2 Benfotiamine Reduces Inflammatory Response in diabetic mouse model

The effect of BFT on inflammation was checked by analyzing the gene expression of anti-inflammatory cytokine i.e. IL-10 and pro-inflammatory cytokine i.e. IL-6 at the wound site in diabetic mice. It was hypothesized that BFT would lower the inflammation by enhancing the release of anti-inflammatory cytokines i.e. IL-10 and lowering the IL-6 level at the wound site. 0.1% BFT dose shows that BFT has an anti-inflammatory response as the IL-6 level decreased while IL-10 levels significantly increased in this group. Figure 3.5A shows that the IL-6 level is significantly downregulated in the vehicle and 0.05% BFT group, and significantly upregulated in the vehicle and 0.05% BFT group on day 7, while 0.1% BFT group shows significant upregulation on days 3 and 7. On day 10, the IL-6 level is significantly upregulated in the vehicle group, and significantly downregulated in the 0.05% BFT group and 0.1% BFT group.

Figure 3.5B shows that the IL-10 level is significantly downregulated in the vehicle and 0.05% BFT group on days 3 and 7, and slight upregulation on day 10, While the 0.1% BFT group shows significant upregulation on days 7 and 10.

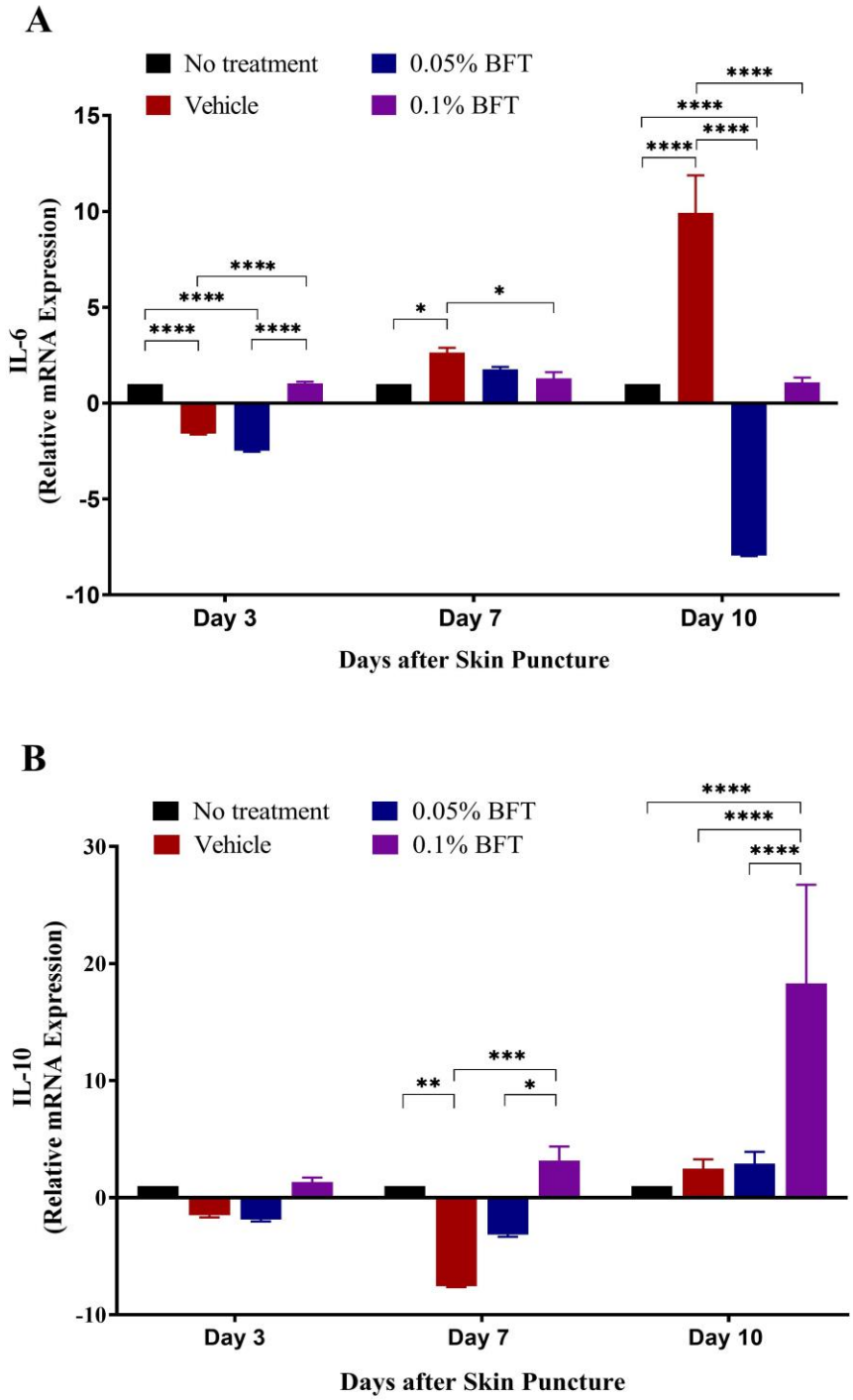

Figure 3. 5: Benfotiamine effect on IL-6 and IL-10 levels

Graphical representation of mRNA expression of (A) IL-6, and (B) IL-10 on days 3, 7, and 10 wounded skin samples of all groups. All the data was statistically analyzed by one-way ANOVA and is presented as mean ± SD. ****$p < 0.0001$, ***$p < 0.001$, **$p < 0.01$, *$p < 0.05$ vs No treatment group.

3.4 Effect of Benfotiamine on Different Biochemical Parameters

3.4.1 Benfotiamine Reduced Oxidative Stress in Diabetic Mouse Model

3.4.1.1 ROS Level

The effect of benfotiamine on oxidative stress was evaluated by measuring the ROS level in BALB/c wild-type diabetic mice in the four groups: No treatment (Control), Vehicle, 0.05% BFT, and 0.1% BFT on days 3, 7, and 10. The results were evaluated by total protein concentrations (ug/uL protein). Results show that ROS level is significantly decreased in 0.05% BFT and 0.1% BFT groups compared to the No treatment and Vehicle group. By day 7, though there is no significant decrease in ROS level, comparatively there is a decrease in ROS in 0.05% BFT and 0.1% BFT groups. On day 10, there was a significant decrease in ROS level in the 0.1% BFT group, and no difference in the 0.05% BFT group on that day compared to the No treatment group and Vehicle group (Figure 3.6).

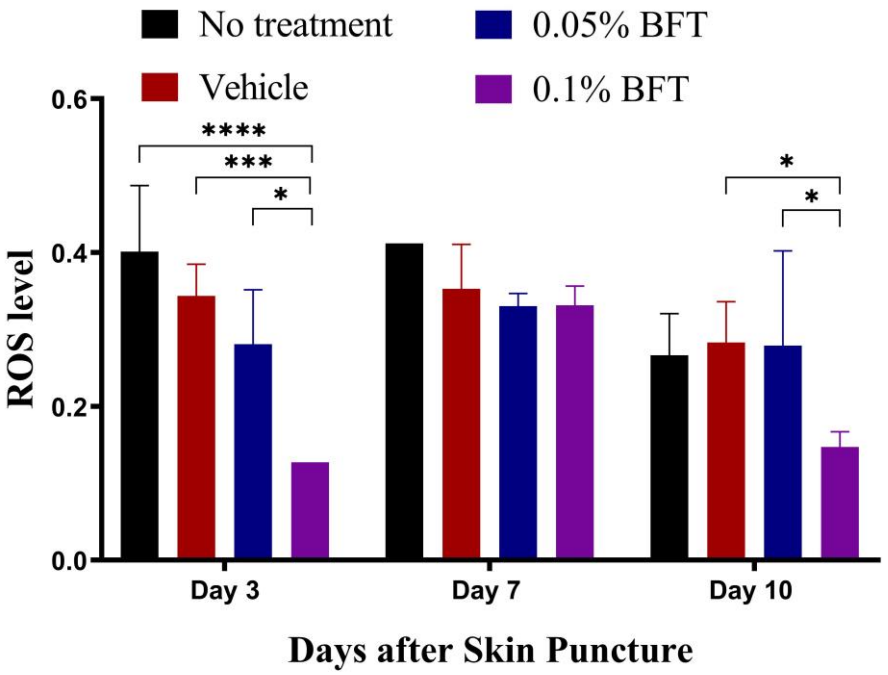

Figure 3. 6: Effect of BFT on oxidative stress

Effect of BFT on ROS on Days 3, 7, and 10 of wounded skin samples of all groups. All the data was statistically analyzed by one-way ANOVA and is presented as mean ± SD. ****$p < 0.0001$, ***$p < 0.001$, *$p < 0.05$ vs No treatment group and Vehicle group.

3.4.2 Benfotiamine Exerts Antioxidant Effect in Diabetic Mouse Model

To check the antioxidant effect of BFT, SOD and Catalase activity was observed.

3.4.2.1 Superoxide Dismutase Activity

The effect of benfotiamine on SOD activity was measured in BALB/c wild-type diabetic mice in the four groups: No treatment (Control), Vehicle, 0.05% BFT, and 0.1% BFT on days 3, 7, and 10. Results show that on day 3 there is a significant increase in SOD activity in the 0.05% BFT group, but a decrease in the 0.1% BFT group compared to the no treatment and Vehicle group. While on days 7 and 10, there is a significant increase in SOD activity was observed in 0.05% BFT and 0.1% BFT groups and decreased in no treatment and vehicle groups (Figure 3.7A).

3.4.2.2 Catalase Activity

Another enzyme that is also antioxidant, Catalase, activity was also measured in BALB/c wild-type diabetic mice in the four groups: No treatment (Control), Vehicle, 0.05% BFT, and 0.1% BFT on days 3, 7, and 10. On day 3, there is no difference in the enzyme activity of all the groups. While, on day 7, the 0.1% BFT group show a significant increase in Catalase activity. By day 10, the 0.05% BFT and 0.1% BFT groups significantly increased this antioxidant enzyme activity (Figure 3.7B).

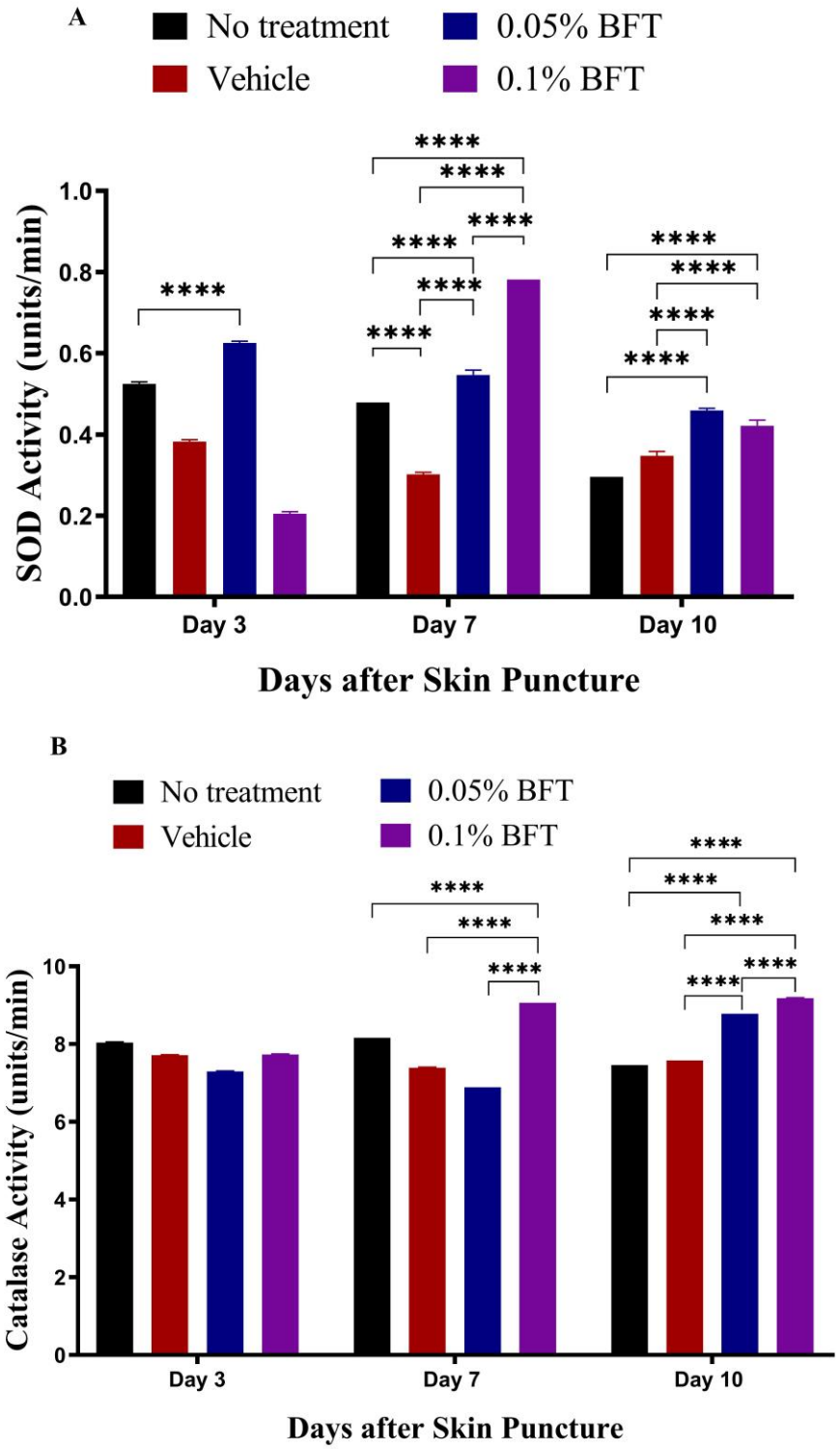

Figure 3. 7: Effect of BFT on antioxidative enzymes activity

Effect of BFT on (A) SOD and (B) Cat enzymes activity on Day 3, Day 7, and Day 10 of wounded skin samples of all groups. All the data was statistically analyzed by one-way ANOVA and is presented as mean ± SD. ****$p < 0.0001$ vs No treatment and Vehicle group.

CHAPTER 4: DISCUSSION

Diabetes mellitus is a group of metabolic disorders, characterized by high blood glucose levels, resulting from insufficient insulin production or impaired bodily response to insulin [115]. The development and progression of DM lead to serious diabetic complications, notably chronic diabetic wounds, which, if left untreated, can result in severe outcomes, such as amputation (Zhang, Li et al. 2023). It is estimated that Type 2 Diabetes Mellitus is the cause of 75% of the one million annual leg amputations worldwide, highlighting the critical need for efficient interventions to address this serious health issue [28]. For efficient wound healing, various cells need to work coordinately to restore damaged skin. The complex pathophysiological link between impaired wound healing and diabetes involves multiple factors [116]. In diabetic wounds, significant oxidative stress and mitochondrial dysfunction are observed [29]. The continuous elevation of blood glucose levels impairs mitochondrial function, increases ROS levels, and induces damage to mitochondrial DNA, thereby contributing to a delayed wound-healing process [30, 31]. This study aimed to identify a novel potential therapeutic agent capable of augmenting the healing in wounded diabetic mice models. Benfotiamine was used to investigate its wound-healing properties in diabetic mice. Benfotiamine exhibits antioxidant and anti-inflammatory properties that participate in the amelioration of diabetic complications [101, 103]. In hyperglycaemic conditions, benfotiamine markedly enhances glucose oxidation and promotes the absorption of glucose [104].

Two different concentrations (0.05% BFT, 0.1% BFT) were used to check the effect of benfotiamine on diabetic wound healing, in comparison to mice treated with vehicle (Vehicle group) and mice received no treatment at all (No treatment group). Benfotiamine showed wound-healing effects *in vivo*, especially in the 0.1% BFT-treated group as compared to other groups. The digital photographs taken from day 0 to day 10 showed significant results (Figure 3.1A). Data show that benfotiamine is involved in improving diabetic wound conditions. Then downstream targets of benfotiamine were checked to know the mechanisms by which it involves in diabetic wound healing. The primary reason for delayed wound healing in diabetic mice is oxidative stress and inflammation that leads to mitochondrial dysfunction and other complications.

In hyperglycemic conditions, an increase in skin glucose level leads to the upregulation of Trisk95 that binds to the RyR receptors of SR and blocks the calcium exchange between

cytoplasm and SR, which in turn leads to the SR calcium overload, increasing the calcium influx into the mitochondria [1]. Calcium is a second messenger, critical in almost all unicellular and metazoan cells. It involves different physiological activities including mitochondrial bioenergetics [117, 118]. Elevated calcium leads to mitochondrial calcium overload, a prerequisite to open permeability transition pores (PTP), mitochondrial swelling, and necrotic cell death [119]. This calcium overload increases the permeability of the mitochondrial membrane, and the leakage of cytochrome C from the mitochondria, leading to mitochondria-induced apoptosis.

In the current study, it is observed that benfotiamine downregulates the Trisk95 level in wounded diabetic mice (Figure 3.3) and this downregulation is dose-dependent. On day 3 Trisk95 level is consistent in all the groups, indicating a similar initial response to the diabetic environment. However, there is a significant upregulation of Trisk95 in the vehicle group on day 7, suggesting exacerbations of hyperglycemic conditions in this group. In the 0.1% BFT group, there is significant downregulation of Trisk95 on day 7 compared to the vehicle group, indicating that BFT may mitigate hyperglycemia-induced stress in the skin. Despite these changes, a higher level of Trisk95 in all the groups on day 7 compared to day 3, may show the general progression of hyperglycemia in the diabetic environment. By day 10, the vehicle group shows continued significant upregulation of Trisk95, further indicating the worsening of hyperglycaemic conditions in this group. Both 0.05% BFT and 0.1% BFT groups show significant downregulation of Trisk95 and the 0.05% BFT dose shows a more significant downregulation of Tris95 on day 10. This suggests that BFT effectively reduces hyperglycemia-induced stress over time, potentially improving calcium signaling and reducing mitochondrial fragmentation, which is crucial for better wound healing. The observed downregulation of Trisk95 in the treatment groups justifies the therapeutic potential of BFT in managing hyperglycemia-related complications in diabetic wound healing. As Trisk95 is involved in calcium influx into the mitochondria, benfotiamine may be involved in restoring calcium-related mitochondrial dysfunction. It is evident that benfotiamine restores hyperglycemia-induced disruption in calcium homeostasis in diabetic mice [120].

Calcium signaling is essential in ROS production, when calcium is overloaded it leads to the production of ROS [121]. ROS is important in overcoming microbial invasion and regulating intracellular signaling pathways under normal physiological conditions, which alter the wound-healing process [122]. Excessive oxidative stress can damage cells' DNA, lipids, and proteins,

which may ultimately result in cell death and subsequent tissue damage [123]. ROS has harmful effects on cellular homeostasis, including a decrease in antioxidant defenses, which increases the redox imbalance. Clinical research has demonstrated that wound tissue in diabetic patients experiences more severe oxidative stress than nondiabetic wounded skin tissue [124]. In the skin, diabetic rats have reduced levels of superoxide dismutase, and catalase activity, and an overall decrease in antioxidant status [125]. Superoxide dismutase (SOD), an antioxidant enzyme, plays a critical role in oxidative stress. SOD catalyzes the conversion of superoxide radicals into hydrogen peroxide [126]. Catalase, another important enzyme, is localized in peroxisomes and catalyzes the breakdown of hydrogen peroxide (H_2O_2) into water and oxygen, further contributing to the reduction of oxidative stress [127]. However, in diabetic wound healing, SOD is often expressed at insufficient levels, leading to increased oxidative stress and impaired wound repair. Application of SOD in diabetic wound healing can significantly improve chronic diabetic wound repair [128].

This study indicates the effect of BFT on oxidative stress in diabetic wound healing. ROS level was significantly downregulated in the 0.05%BFT group on day 3, suggesting an early antioxidant effect of BFT. However, on day 7, there was no significant downregulation of ROS in any group, indicating a temporary stabilization of oxidative stress. By day 10, both the 0.05%BFT and 0.1%BFT groups showed significant downregulation of ROS, reflecting a sustained reduction in oxidative stress, particularly with prolonged treatment.

SOD activity showed a significant increase on day 3 in the Low dose group, but a marked decrease in activity in the 0.1%BFT group, possibly indicating an initial oxidative response at lower doses. Interestingly, by day 7, there was a significant increase in SOD activity in both groups, with this trend continuing significantly on day 10, suggesting that BFT enhances the antioxidant defense over time, particularly at higher doses. For catalase, there was no difference in activity observed on day 3. However, by day 7, catalase activity significantly increased in the 0.1%BFT group, and by day 10, it was significantly elevated in both the 0.05%BFT and 0.1%BFT groups. This pattern indicates that BFT may enhance the enzymatic antioxidant defenses, particularly in the later stages of wound healing. These results suggest that BFT, especially at higher doses, effectively modulates oxidative stress by regulating ROS levels and enhancing the activity of key antioxidant enzymes like SOD and catalase, thereby potentially improving wound healing in diabetic conditions.

Proinflammatory cytokines are essential for initiating wound healing, any upregulation of IL-1ß, TNF-α, IL-6, TGF-ß, and CRP and downregulation of IL-10, leads to a detrimental environment for the healing process [129]. IL-6 is important for acute inflammation and timely wound healing [130, 131]. Released early after injury, IL-6 stimulates the release of pro-inflammatory cytokines from tissue-resident macrophages, keratinocytes, endothelial cells, and stromal cells. It also promotes leukocyte chemotaxis to the wound site, enabling the inflammatory response [132]. In dermal fibroblasts, IL-6 stimulates collagen production and procollagen gene expression [130], involved in wound re-epithelialization by creating the collagen and fibronectin scaffold [133]. Consequently, IL-6 gene knockout may delay re-epithelialization, potentially via TGF-β1 signaling [130], leading to delayed and poorly healed wounds [134]. IL-6 also induces angiogenesis by stimulating VEGF production. During normal wound repair, IL-6 expression significantly decreases during the remodeling phase, likely due to the apoptosis of infiltrating inflammatory leukocytes and the subsequent reduction in cytokine signaling [135]. This reduction is critical for transitioning the wound bed from a chronic inflammation to a reparative one. Dysregulated IL-6 signaling, can lead to a prolonged proliferative phase, excessive collagen deposition, and the formation of hypertrophic scar [135]. Such dysregulation is commonly observed in various diabetic complications, where altered IL-6 levels contribute to the chronic inflammation associated with non-healing diabetic ulcers [136]. IL-6 also regulates M2 macrophage polarization, possibly by upregulating the IL-4 receptor. M2 macrophages play a crucial role in late-stage wound repair, producing anti-inflammatory cytokines like TGF-β and IL-10 [132]. Overexpression of IL-10 in postnatal cutaneous dermal wounds promotes regenerative, scarless tissue repair by regulating inflammation and promoting an extracellular wound matrix formation that is rich in hyaluronan via fibroblast activity. This hyaluronan-rich matrix is essential to support the regenerative wound-healing ability of IL-10. Additionally, IL-10 modulates the synthesis and degradation of several extracellular matrix molecules in different fibroblast cell types, thereby maintaining its anti-fibrotic effects during skin wound healing. Furthermore, IL-10 overexpression is key in promoting neovascularization and enhancing healing in both normal and diabetic conditions. In diabetic mice, higher levels of IL-10 significantly improve wound healing outcomes by enhancing the recruitment and retention of endothelial progenitor cells (EPCs) at the injury site, leading to increased capillary lumen density within the wound [137]. Increased neutrophils and inflammatory cytokines like IL-6, enhance the activity of NOx, resulting in ROS production [138], and excessive stress during inflammation, leading to damage in the surrounding cells, tissues, and fibroblasts [139].

To check if benfotiamine alleviates this prolonged inflammation, IL-6 and IL-10 expressions were checked in the wounded skin tissue of diabetic mice. Results in Figure 3.2 show that 0.1% BFT dose has more therapeutic effect, leading to a significant upregulation in anti-inflammatory IL-10 gene expression that may be crucial for promoting wound healing and resoluting inflammation and tissue repair. While IL-6 although has proinflammatory properties, is crucial in the early stages of wound healing as it recruits immune cells to the wound site. Hence, its regulated increase in gene expression on days 3 and 7 shows a proper inflammatory phase that leads the wound to the proliferative phase. Slight upregulation of IL-6 on day 10 in the 0.1% BFT group can be an indication of a finely tuned response that balances the need for both inflammation and its resolution in the context of diabetic wound healing.

These findings suggest that benfotiamine, especially 0.1% BFT dose, can potentially improve wound healing in diabetic mice. As benfotiamine downregulates the Trisk95 expression that in turn may mitigate the hyperglycemia-induced stress condition, reducing calcium influx into the mitochondria and preventing mitochondrial fragmentation. It also improves the antioxidant defense system by decreasing ROS levels and increasing antioxidant enzymes; and shows an anti-inflammatory response by downregulating the IL-6 and upregulating the IL-10 expression, which are critical for normal diabetic wound healing. This improved antioxidant defense and anti-inflammatory response may reduce mitochondrial dysfunction and mitochondrial-induced apoptosis.

Despite the valuable findings, the study has a few notable limitations, such as potential interactions with other medications commonly used in diabetic patients were not investigated, which could affect the BFT's real-world applicability. We assessed trisk95 levels, inflammatory response, and antioxidant effects, but did not directly measure calcium signaling, mitochondrial function, or apoptosis, leaving gaps in fully understanding BFT impact on these key mechanisms in wound healing. Moreover, environmental factors such as diet or stress, which can influence wound healing, may not have been fully controlled or accounted for in this study.

CHAPTER 5: CONCLUSION AND FUTURE RECOMMENDATIONS

This study demonstrates that BFT effectively downregulates Trisk95 expression, a gene associated with hyperglycemia-induced cellular stress, and has an anti-inflammatory and antioxidant effect. This suggests that BFT helps in diabetic wound healing by improving calcium signaling and mitochondrial function. These findings highlight the potential of benfotiamine as a therapeutic agent for improving wound healing in diabetic conditions. This research contributes to a deeper understanding of the molecular mechanisms involved in diabetic wound healing and opens new possibilities for therapeutic intervention. However, further studies are needed to fully elucidate the underlying mechanisms and to determine whether these effects translate into long-term improvements in wound healing outcomes. Future studies should focus on predicting the molecular target of BFT for wound healing and the anti-diabetic viability of BFT.

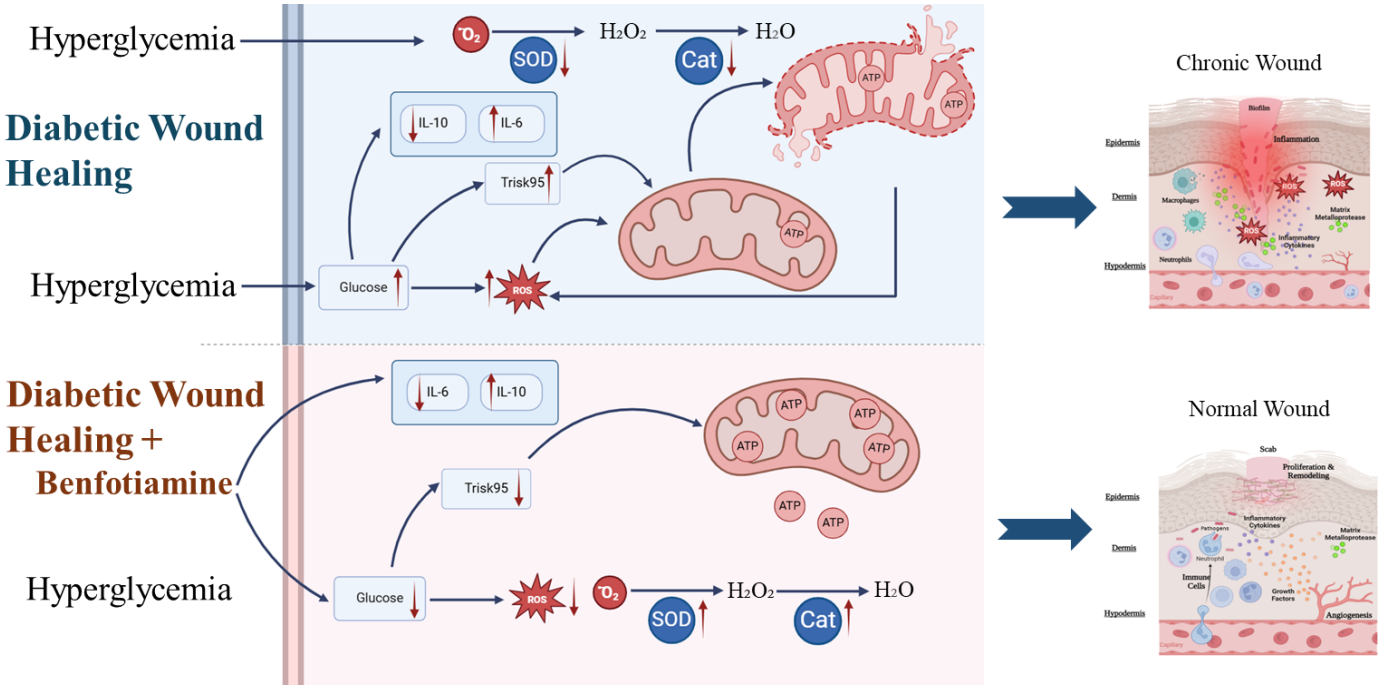

Figure 5. 1: Visual summary of key conclusions

REFERENCES

[1] N. Ali *et al.*, "Trisk 95 as a novel skin mirror for normal and diabetic systemic glucose level," vol. 10, no. 1, p. 12246, 2020.

[2] A. Slominski and J. J. E. r. Wortsman, "Neuroendocrinology of the skin," vol. 21, no. 5, pp. 457-487, 2000.

[3] R. Nejati, D. Kovacic, and A. J. E. r. o. d. Slominski, "Neuro-immune-endocrine functions of the skin: an overview," vol. 8, no. 6, pp. 581-583, 2013.

[4] S. A. Eming, P. Martin, and M. J. S. t. m. Tomic-Canic, "Wound repair and regeneration: mechanisms, signaling, and translation," vol. 6, no. 265, pp. 265sr6-265sr6, 2014.

[5] M. B. Dreifke, A. A. Jayasuriya, A. C. J. M. S. Jayasuriya, and E. C, "Current wound healing procedures and potential care," vol. 48, pp. 651-662, 2015.

[6] S. Zhong, Y. Zhang, C. J. W. I. R. N. Lim, and Nanobiotechnology, "Tissue scaffolds for skin wound healing and dermal reconstruction," vol. 2, no. 5, pp. 510-525, 2010.

[7] H. R. Lee *et al.*, "Liquid plasma as a treatment for cutaneous wound healing through regulation of redox metabolism," vol. 14, no. 2, p. 119, 2023.

[8] S. a. Guo and L. A. J. J. o. d. r. DiPietro, "Factors affecting wound healing," vol. 89, no. 3, pp. 219-229, 2010.

[9] A. Gosain and L. A. J. W. j. o. s. DiPietro, "Aging and wound healing," vol. 28, pp. 321-326, 2004.

[10] I. George Broughton, J. E. Janis, C. E. J. P. Attinger, and r. surgery, "The basic science of wound healing," vol. 117, no. 7S, pp. 12S-34S, 2006.

[11] L. Cañedo-Dorantes and M. J. I. j. o. i. Cañedo-Ayala, "Skin acute wound healing: a comprehensive review," vol. 2019, 2019.

[12] I. George Broughton, J. E. Janis, C. E. J. P. Attinger, and r. surgery, "Wound healing: an overview," vol. 117, no. 7S, pp. 1e-S-32e-S, 2006.

[13] K. Geng *et al.*, "High glucose-induced STING activation inhibits diabetic wound healing through promoting M1 polarization of macrophages," vol. 9, no. 1, p. 136, 2023.

[14] P. J. C. d. d. t. Modi, "Diabetes beyond insulin: review of new drugs for treatment of diabetes mellitus," vol. 4, no. 1, pp. 39-47, 2007.

[15] J. E. Shaw, R. A. Sicree, P. Z. J. D. r. Zimmet, and c. practice, "Global estimates of the prevalence of diabetes for 2010 and 2030," vol. 87, no. 1, pp. 4-14, 2010.

[16] V. J. T. L. Falanga, "Wound healing and its impairment in the diabetic foot," vol. 366, no. 9498, pp. 1736-1743, 2005.

[17] M. Peppa, P. Stavroulakis, S. A. J. W. R. Raptis, and Regeneration, "Advanced glycoxidation products and impaired diabetic wound healing," vol. 17, no. 4, pp. 461-472, 2009.

[18] S. Narayanan *et al.*, "HypoxamiR-210 accelerates wound healing in diabetic mice by improving cellular metabolism," vol. 3, no. 1, p. 768, 2020.

[19] A. J. Boulton *et al.*, "Diagnosis and management of diabetic foot infections," 2020.

[20] D. G. Armstrong and G. C. J. N. R. E. Gurtner, "A histologically hostile environment made more hospitable?," vol. 14, no. 9, pp. 511-512, 2018.

[21] R. Ali, T. Khamis, G. Enan, G. El-Didamony, B. Sitohy, and G. J. M. Abdel-Fattah, "The healing capability of clove flower extract (CFE) in streptozotocin-induced (STZ-induced) diabetic rat wounds infected with multidrug resistant bacteria," vol. 27, no. 7, p. 2270, 2022.

[22] Q. Li *et al.*, "Heme oxygenase-1 alleviates advanced glycation end product-induced oxidative stress, inflammatory response and biological behavioral disorders in rat dermal fibroblasts," vol. 22, no. 5, pp. 1-11, 2021.
[23] M. Teng *et al.*, "Development of tannin-bridged cerium oxide microcubes-chitosan cryogel as a multifunctional wound dressing," vol. 214, p. 112479, 2022.
[24] M. J. N. Brownlee, "Biochemistry and molecular cell biology of diabetic complications," vol. 414, no. 6865, pp. 813-820, 2001.
[25] T. Nishikawa, D. Edelstein, and M. J. K. I. Brownlee, "The missing link: a single unifying mechanism for diabetic complications," vol. 58, pp. S26-S30, 2000.
[26] J. Suarez, Y. Hu, A. Makino, E. Fricovsky, H. Wang, and W. H. J. A. J. o. P.-C. P. Dillmann, "Alterations in mitochondrial function and cytosolic calcium induced by hyperglycemia are restored by mitochondrial transcription factor A in cardiomyocytes," vol. 295, no. 6, pp. C1561-C1568, 2008.
[27] J. H. Kim *et al.*, "High levels of oxidative stress and skin microbiome are critical for initiation and development of chronic wounds in diabetic mice," vol. 9, no. 1, p. 19318, 2019.
[28] M. Naseeb *et al.*, "Rutin Promotes Wound Healing by Inhibiting Oxidative Stress and Inflammation in Metformin-Controlled Diabetes in Rats," 2024.
[29] G. Jiang *et al.*, "Mitochondrial dysfunction and oxidative stress in diabetic wound," p. e23407, 2023.
[30] M. Cano Sanchez, S. Lancel, E. Boulanger, and R. J. A. Neviere, "Targeting oxidative stress and mitochondrial dysfunction in the treatment of impaired wound healing: a systematic review," vol. 7, no. 8, p. 98, 2018.
[31] Z. Zhang, Q. Huang, D. Zhao, F. Lian, X. Li, and W. J. F. i. E. Qi, "The impact of oxidative stress-induced mitochondrial dysfunction on diabetic microvascular complications," vol. 14, p. 1112363, 2023.
[32] A. B. J. W. r. Lansdown and regeneration, "Calcium: a potential central regulator in wound healing in the skin," vol. 10, no. 5, pp. 271-285, 2002.
[33] S. Xu and A. D. J. D. c. Chisholm, "C. elegans epidermal wounding induces a mitochondrial ROS burst that promotes wound repair," vol. 31, no. 1, pp. 48-60, 2014.
[34] J. Law, S. Chowdhury, B. Aminuddin, and B. J. R. R. Ruszymah, "Effect of calcium concentration on keratinocute differentiation in 2-D culture and 3-D construct," vol. 4, no. 1, pp. 22-9, 2015.
[35] M. Xue and C. J. J. A. i. w. c. Jackson, "Extracellular matrix reorganization during wound healing and its impact on abnormal scarring," vol. 4, no. 3, pp. 119-136, 2015.
[36] W. Razzell, I. R. Evans, P. Martin, and W. J. C. B. Wood, "Calcium flashes orchestrate the wound inflammatory response through DUOX activation and hydrogen peroxide release," vol. 23, no. 5, pp. 424-429, 2013.
[37] M. J. Berridge, M. D. Bootman, and P. J. N. Lipp, "Calcium-a life and death signal," vol. 395, no. 6703, pp. 645-648, 1998.
[38] T. Subramaniam, M. B. Fauzi, Y. Lokanathan, and J. X. J. I. J. o. M. S. Law, "The role of calcium in wound healing," vol. 22, no. 12, p. 6486, 2021.
[39] J. Szymański *et al.*, "Interaction of mitochondria with the endoplasmic reticulum and plasma membrane in calcium homeostasis, lipid trafficking and mitochondrial structure," vol. 18, no. 7, p. 1576, 2017.
[40] S. Romero-Garcia and H. J. I. j. o. o. Prado-Garcia, "Mitochondrial calcium: Transport and modulation of cellular processes in homeostasis and cancer," vol. 54, no. 4, pp. 1155-1167, 2019.
[41] K. J. Kamer *et al.*, "MICU1 imparts the mitochondrial uniporter with the ability to discriminate between Ca2+ and Mn2+," vol. 115, no. 34, pp. E7960-E7969, 2018.

[42] Y. Xing *et al.*, "Dimerization of MICU proteins controls Ca2+ influx through the mitochondrial Ca2+ uniporter," vol. 26, no. 5, pp. 1203-1212. e4, 2019.
[43] N. Nemani, S. Shanmughapriya, and M. J. C. C. Madesh, "Molecular regulation of MCU: Implications in physiology and disease," vol. 74, pp. 86-93, 2018.
[44] F. Fieni, S. Bae Lee, Y. N. Jan, and Y. J. N. c. Kirichok, "Activity of the mitochondrial calcium uniporter varies greatly between tissues," vol. 3, no. 1, p. 1317, 2012.
[45] D. Matuz-Mares, M. González-Andrade, M. G. Araiza-Villanueva, M. M. Vilchis-Landeros, and H. J. A. Vázquez-Meza, "Mitochondrial calcium: effects of its imbalance in disease," vol. 11, no. 5, p. 801, 2022.
[46] S. Marchi *et al.*, "Mitochondrial and endoplasmic reticulum calcium homeostasis and cell death," vol. 69, pp. 62-72, 2018.
[47] J. J. C. d. Rieusset and disease, "The role of endoplasmic reticulum-mitochondria contact sites in the control of glucose homeostasis: an update," vol. 9, no. 3, p. 388, 2018.
[48] C. Giorgi, D. De Stefani, A. Bononi, R. Rizzuto, P. J. T. i. j. o. b. Pinton, and c. biology, "Structural and functional link between the mitochondrial network and the endoplasmic reticulum," vol. 41, no. 10, pp. 1817-1827, 2009.
[49] N. R. Brandt, A. H. Caswell, S.-R. Wen, and J. A. J. T. J. o. m. b. Talvenheimo, "Molecular interactions of the junctional foot protein and dihydropyridine receptor in skeletal muscle triads," vol. 113, pp. 237-251, 1990.
[50] K. C. Kim, A. H. Caswell, J. A. Talvenheimo, and N. R. J. B. Brandt, "Isolation of a terminal cisterna protein which may link the dihydropyridine receptor to the junctional foot protein in skeletal muscle," vol. 29, no. 39, pp. 9281-9289, 1990.
[51] C. M. Knudson, K. Stang, A. O. Jorgensen, and K. J. J. o. B. C. Campbell, "Biochemical characterization of ultrastructural localization of a major junctional sarcoplasmic reticulum glycoprotein (triadin)," vol. 268, no. 17, pp. 12637-12645, 1993.
[52] S. A. Goonasekera *et al.*, "Triadin binding to the C-terminal luminal loop of the ryanodine receptor is important for skeletal muscle excitation–contraction coupling," vol. 130, no. 4, pp. 365-378, 2007.
[53] J. M. Lee *et al.*, "Negatively charged amino acids within the intraluminal loop of ryanodine receptor are involved in the interaction with triadin," vol. 279, no. 8, pp. 6994-7000, 2004.
[54] L. Zhang, J. Kelley, G. Schmeisser, Y. M. Kobayashi, and L. R. J. J. o. B. C. Jones, "Complex formation between junctin, triadin, calsequestrin, and the ryanodine receptor: proteins of the cardiac junctional sarcoplasmic reticulum membrane," vol. 272, no. 37, pp. 23389-23397, 1997.
[55] I. Marty *et al.*, "Cloning and characterization of a new isoform of skeletal muscle triadin," vol. 275, no. 11, pp. 8206-8212, 2000.
[56] S. S. Rezgui *et al.*, "Triadin (Trisk 95) overexpression blocks excitation-contraction coupling in rat skeletal myotubes," vol. 280, no. 47, pp. 39302-39308, 2005.
[57] I. Marty, M. Robert, M. Ronjat, I. Bally, G. Arlaud, and M. J. B. J. Villaz, "Localization of the N-terminal and C-terminal ends of triadin with respect to the sarcoplasmic reticulum membrane of rabbit skeletal muscle," vol. 307, no. 3, pp. 769-774, 1995.
[58] W. Guo and K. P. J. J. o. B. C. Campbell, "Association of triadin with the ryanodine receptor and calsequestrin in the lumen of the sarcoplasmic reticulum," vol. 270, no. 16, pp. 9027-9030, 1995.
[59] Y. M. Kobayashi, B. A. Alseikhan, and L. R. J. J. o. B. C. Jones, "Localization and characterization of the calsequestrin-binding domain of triadin 1: evidence for a

charged β-strand in mediating the protein-protein interaction," vol. 275, no. 23, pp. 17639-17646, 2000.
[60] S. Oddoux *et al.*, "Triadin deletion induces impaired skeletal muscle function," vol. 284, no. 50, pp. 34918-34929, 2009.
[61] E. Wium, A. F. Dulhunty, and N. A. Beard, "A skeletal muscle ryanodine receptor interaction domain in triadin," 2012.
[62] S. Orrenius, B. Zhivotovsky, and P. J. N. r. M. c. b. Nicotera, "Regulation of cell death: the calcium–apoptosis link," vol. 4, no. 7, pp. 552-565, 2003.
[63] G. Hajnóczky, L. D. Robb-Gaspers, M. B. Seitz, and A. P. J. C. Thomas, "Decoding of cytosolic calcium oscillations in the mitochondria," vol. 82, no. 3, pp. 415-424, 1995.
[64] R. G. J. J. o. b. Hansford and biomembranes, "Physiological role of mitochondrial Ca 2+ transport," vol. 26, pp. 495-508, 1994.
[65] K. M. Holmström and T. J. N. r. M. c. b. Finkel, "Cellular mechanisms and physiological consequences of redox-dependent signalling," vol. 15, no. 6, pp. 411-421, 2014.
[66] P. S. Brookes, Y. Yoon, J. L. Robotham, M. Anders, and S.-S. J. A. J. o. P.-C. P. Sheu, "Calcium, ATP, and ROS: a mitochondrial love-hate triangle," 2004.
[67] B. C. Callaghan, A. A. Little, E. L. Feldman, and R. A. J. C. d. o. s. r. Hughes, "Enhanced glucose control for preventing and treating diabetic neuropathy," no. 6, 2012.
[68] H. J. R. b. Sies, "Oxidative stress: a concept in redox biology and medicine," vol. 4, pp. 180-183, 2015.
[69] M. Schäfer and S. J. P. r. Werner, "Oxidative stress in normal and impaired wound repair," vol. 58, no. 2, pp. 165-171, 2008.
[70] C. K. Sen and S. J. B. e. B. A.-G. S. Roy, "Redox signals in wound healing," vol. 1780, no. 11, pp. 1348-1361, 2008.
[71] J. Dworzański *et al.*, "Glutathione peroxidase (GPx) and superoxide dismutase (SOD) activity in patients with diabetes mellitus type 2 infected with Epstein-Barr virus," vol. 15, no. 3, p. e0230374, 2020.
[72] N. Zhang, B. T. Andresen, and C. J. W. J. o. C. Zhang, "Inflammation and reactive oxygen species in cardiovascular disease," vol. 2, no. 12, p. 408, 2010.
[73] Y. J. F. i. P. Qiao, "Reactive oxygen species in cardiovascular calcification: role of medicinal plants," vol. 13, p. 858160, 2022.
[74] R. Hu *et al.*, "Salidroside ameliorates endothelial inflammation and oxidative stress by regulating the AMPK/NF-κB/NLRP3 signaling pathway in AGEs-induced HUVECs," vol. 867, p. 172797, 2020.
[75] C. Yang *et al.*, "Oxidative stress mediates chemical hypoxia-induced injury and inflammation by activating NF-κb-COX-2 pathway in HaCaT cells," vol. 31, pp. 531-538, 2011.
[76] D. R. Maldaner *et al.*, "In vitro effect of low-level laser therapy on the proliferative, apoptosis modulation, and oxi-inflammatory markers of premature-senescent hydrogen peroxide-induced dermal fibroblasts," vol. 34, pp. 1333-1343, 2019.
[77] Z. Xu *et al.*, "Thermosensitive hydrogel incorporating Prussian blue nanoparticles promotes diabetic wound healing via ROS scavenging and mitochondrial function restoration," vol. 14, no. 12, pp. 14059-14071, 2022.
[78] J. E. Janis, B. J. P. Harrison, and r. surgery, "Wound healing: part I. Basic science," vol. 138, no. 3S, pp. 9S-17S, 2016.
[79] N. Bryan, H. Ahswin, N. Smart, Y. Bayon, S. Wohlert, and J. A. J. E. C. M. Hunt, "Reactive oxygen species (ROS)–a family of fate deciding molecules pivotal in constructive inflammation and wound healing," vol. 24, no. 249, p. e65, 2012.

[80] M. Portou, D. Baker, D. Abraham, and J. J. V. p. Tsui, "The innate immune system, toll-like receptors and dermal wound healing: A review," vol. 71, pp. 31-36, 2015.
[81] A. Kasuya and Y. J. J. o. d. s. Tokura, "Attempts to accelerate wound healing," vol. 76, no. 3, pp. 169-172, 2014.
[82] F. Jiang, Y. Zhang, and G. J. J. P. r. Dusting, "NADPH oxidase-mediated redox signaling: roles in cellular stress response, stress tolerance, and tissue repair," vol. 63, no. 1, pp. 218-242, 2011.
[83] T. Shen, K. Dai, Y. Yu, J. Wang, and C. J. A. b. Liu, "Sulfated chitosan rescues dysfunctional macrophages and accelerates wound healing in diabetic mice," vol. 117, pp. 192-203, 2020.
[84] S. A. Eming, T. Krieg, and J. M. J. J. o. I. D. Davidson, "Inflammation in wound repair: molecular and cellular mechanisms," vol. 127, no. 3, pp. 514-525, 2007.
[85] S. P. Hussain, L. J. Hofseth, and C. C. J. N. R. C. Harris, "Radical causes of cancer," vol. 3, no. 4, pp. 276-285, 2003.
[86] E. Galkina and K. J. A. r. o. i. Ley, "Immune and inflammatory mechanisms of atherosclerosis," vol. 27, no. 1, pp. 165-197, 2009.
[87] Y. Yamada, Y. Takano, Satrialdi, J. Abe, M. Hibino, and H. J. B. Harashima, "Therapeutic strategies for regulating mitochondrial oxidative stress," vol. 10, no. 1, p. 83, 2020.
[88] D. C. J. A. R. C. D. B. Chan, "Mitochondrial fusion and fission in mammals," vol. 22, no. 1, pp. 79-99, 2006.
[89] R. J. Youle and A. M. J. S. Van Der Bliek, "Mitochondrial fission, fusion, and stress," vol. 337, no. 6098, pp. 1062-1065, 2012.
[90] T. Pathak, M. J. P. Trebak, and therapeutics, "Mitochondrial Ca2+ signaling," vol. 192, pp. 112-123, 2018.
[91] B. J. T. J. o. c. b. Mesmin, "Mitochondrial lipid transport and biosynthesis: a complex balance," vol. 214, no. 1, p. 9, 2016.
[92] P. Gurung, J. R. Lukens, and T.-D. J. T. i. m. m. Kanneganti, "Mitochondria: diversity in the regulation of the NLRP3 inflammasome," vol. 21, no. 3, pp. 193-201, 2015.
[93] N. S. Chandel *et al.*, "Reactive oxygen species generated at mitochondrial complex III stabilize hypoxia-inducible factor-1α during hypoxia: a mechanism of O2 sensing," vol. 275, no. 33, pp. 25130-25138, 2000.
[94] J. L. Jacobs and C. B. J. J. o. m. b. Coyne, "Mechanisms of MAVS regulation at the mitochondrial membrane," vol. 425, no. 24, pp. 5009-5019, 2013.
[95] S. Marchi, E. Guilbaud, S. W. Tait, T. Yamazaki, and L. J. N. R. I. Galluzzi, "Mitochondrial control of inflammation," vol. 23, no. 3, pp. 159-173, 2023.
[96] H. Rizwan, S. Pal, S. Sabnam, and A. J. L. s. Pal, "High glucose augments ROS generation regulates mitochondrial dysfunction and apoptosis via stress signalling cascades in keratinocytes," vol. 241, p. 117148, 2020.
[97] X. Wang *et al.*, "Hypoxic preconditioning combined with curcumin promotes cell survival and mitochondrial quality of bone marrow mesenchymal stem cells, and accelerates cutaneous wound healing via PGC-1α/SIRT3/HIF-1α signaling," vol. 159, pp. 164-176, 2020.
[98] J. Y. Baek *et al.*, "Protective role of mitochondrial peroxiredoxin III against UVB-induced apoptosis of epidermal keratinocytes," vol. 137, no. 6, pp. 1333-1342, 2017.
[99] M.-L. Volvert *et al.*, "Benfotiamine, a synthetic S-acyl thiamine derivative, has different mechanisms of action and a different pharmacological profile than lipid-soluble thiamine disulfide derivatives," vol. 8, pp. 1-11, 2008.
[100] I. Bozic and I. J. H. Lavrnja, "Thiamine and benfotiamine: Focus on their therapeutic potential," vol. 9, no. 11, 2023.

[101] U. Schmid, H. Stopper, A. Heidland, N. J. D. m. r. Schupp, and reviews, "Benfotiamine exhibits direct antioxidative capacity and prevents induction of DNA damage in vitro," vol. 24, no. 5, pp. 371-377, 2008.
[102] I. Bozic, D. Savic, I. Stevanovic, S. Pekovic, N. Nedeljkovic, and I. J. F. i. c. n. Lavrnja, "Benfotiamine upregulates antioxidative system in activated BV-2 microglia cells," vol. 9, p. 351, 2015.
[103] P. Balakumar, A. Rohilla, P. Krishan, P. Solairaj, and A. J. P. r. Thangathirupathi, "The multifaceted therapeutic potential of benfotiamine," vol. 61, no. 6, pp. 482-488, 2010.
[104] D. Fraser *et al.*, "Benfotiamine increases glucose oxidation and downregulates NADPH oxidase 4 expression in cultured human myotubes exposed to both normal and high glucose concentrations," vol. 7, no. 3, pp. 459-469, 2012.
[105] M. Shoeb, K. V. J. F. R. B. Ramana, and Medicine, "Anti-inflammatory effects of benfotiamine are mediated through the regulation of the arachidonic acid pathway in macrophages," vol. 52, no. 1, pp. 182-190, 2012.
[106] R. G. Katare, A. Caporali, A. Oikawa, M. Meloni, C. Emanueli, and P. J. C. H. F. Madeddu, "Vitamin B1 analog benfotiamine prevents diabetes-induced diastolic dysfunction and heart failure through Akt/Pim-1–mediated survival pathway," vol. 3, no. 2, pp. 294-305, 2010.
[107] M. S. Huijberts, N. C. Schaper, C. G. J. D. m. r. Schalkwijk, and reviews, "Advanced glycation end products and diabetic foot disease," vol. 24, no. S1, pp. S19-S24, 2008.
[108] Y. Kohda, M. Kanematsu, T. Kono, F. Terasaki, and T. J. J. o. p. s. Tanaka, "Protein O-glycosylation induces collagen expression and contributes to diabetic cardiomyopathy in rat cardiac fibroblasts," vol. 111, no. 4, pp. 446-450, 2009.
[109] H.-P. Hammes *et al.*, "Benfotiamine blocks three major pathways of hyperglycemic damage and prevents experimental diabetic retinopathy," vol. 9, no. 3, pp. 294-299, 2003.
[110] S.-H. Oh *et al.*, "Detection of transketolase in bone marrow–derived insulin-producing cells: benfotiamine enhances insulin synthesis and glucose metabolism," vol. 18, no. 1, pp. 37-46, 2009.
[111] E. Beltramo, E. Berrone, S. Buttiglieri, M. J. D. M. R. Porta, and Reviews, "Thiamine and benfotiamine prevent increased apoptosis in endothelial cells and pericytes cultured in high glucose," vol. 20, no. 4, pp. 330-336, 2004.
[112] E. Berrone, E. Beltramo, C. Solimine, A. U. Ape, and M. J. J. o. B. C. Porta, "Regulation of intracellular glucose and polyol pathway by thiamine and benfotiamine in vascular cells cultured in high glucose," vol. 281, no. 14, pp. 9307-9313, 2006.
[113] R. Babaei-Jadidi, N. Karachalias, N. Ahmed, S. Battah, and P. J. J. D. Thornalley, "Prevention of incipient diabetic nephropathy by high-dose thiamine and benfotiamine," vol. 52, no. 8, pp. 2110-2120, 2003.
[114] R. A. Baum and F. L. J. N. C. i. a. C. W. Iber, "Thiamin—the interaction of aging, alcoholism, and malabsorption in various populations," vol. 44, pp. 85-116, 1984.
[115] H. Jin *et al.*, "Melatonin protects endothelial progenitor cells against AGE-induced apoptosis via autophagy flux stimulation and promotes wound healing in diabetic mice," vol. 50, no. 11, pp. 1-15, 2018.
[116] S. Bibi, F. Ahmad, M. R. Alam, M. Ansar, K. S. Yeou, and H. M. J. I. J. o. P. R. I. Wahedi, "Lapachol-Induced Upregulation of Sirt1/Sirt3 is linked with Improved Skin Wound Healing in Alloxan-induced Diabetic Mice," vol. 20, no. 3, p. 419, 2021.
[117] J. Soboloff, B. S. Rothberg, M. Madesh, and D. L. J. N. r. M. c. b. Gill, "STIM proteins: dynamic calcium signal transducers," vol. 13, no. 9, pp. 549-565, 2012.

[118] M. J. Berridge, M. D. Bootman, and H. L. J. N. r. M. c. b. Roderick, "Calcium signalling: dynamics, homeostasis and remodelling," vol. 4, no. 7, pp. 517-529, 2003.
[119] D. G. J. C. c. Nicholls, "Mitochondria and calcium signaling," vol. 38, no. 3-4, pp. 311-317, 2005.
[120] V. Serhiyenko, M. Hotsko, O. Snitynska, and A. J. M. Serhiyenko, "Benfotiamine and type 2 diabetes mellitus," vol. 7, p. 00200, 2018.
[121] A. Gordeeva, R. Zvyagilskaya, and Y. A. J. B. Labas, "Cross-talk between reactive oxygen species and calcium in living cells," vol. 68, pp. 1077-1080, 2003.
[122] A. Jindam, V. G. Yerra, and A. J. A. o. t. m. Kumar, "Nrf2: a promising trove for diabetic wound healing," vol. 5, no. 23, 2017.
[123] O. Tabak *et al.*, "Oxidative lipid, protein, and DNA damage as oxidative stress markers in vascular complications of diabetes mellitus," vol. 34, no. 3, pp. E163-E171, 2011.
[124] M. Long *et al.*, "An essential role of NRF2 in diabetic wound healing," vol. 65, no. 3, pp. 780-793, 2016.
[125] J. A. David, W. J. Rifkin, P. S. Rabbani, and D. J. J. J. o. d. r. Ceradini, "The Nrf2/Keap1/ARE pathway and oxidative stress as a therapeutic target in type II diabetes mellitus," vol. 2017, no. 1, p. 4826724, 2017.
[126] W. Zhang *et al.*, "Antioxidant therapy and antioxidant-related bionanomaterials in diabetic wound healing," vol. 9, p. 707479, 2021.
[127] T. Kurahashi and J. J. J. o. D. B. Fujii, "Roles of antioxidative enzymes in wound healing," vol. 3, no. 2, pp. 57-70, 2015.
[128] L. Zhang, Y. Ma, X. Pan, S. Chen, H. Zhuang, and S. J. C. p. Wang, "A composite hydrogel of chitosan/heparin/poly (γ-glutamic acid) loaded with superoxide dismutase for wound healing," vol. 180, pp. 168-174, 2018.
[129] S. Nirenjen *et al.*, "Exploring the contribution of pro-inflammatory cytokines to impaired wound healing in diabetes," vol. 14, p. 1216321, 2023.
[130] Z.-Q. Lin, T. Kondo, Y. Ishida, T. Takayasu, and N. J. J. o. L. B. Mukaida, "Essential involvement of IL-6 in the skin wound-healing process as evidenced by delayed wound healing in IL-6-deficient mice," vol. 73, no. 6, pp. 713-721, 2003.
[131] T. Kishimoto, "The biology of interleukin-6," 1989.
[132] B. Z. Johnson, A. W. Stevenson, C. M. Prêle, M. W. Fear, and F. M. J. B. Wood, "The role of IL-6 in skin fibrosis and cutaneous wound healing," vol. 8, no. 5, p. 101, 2020.
[133] T. Nishikai-Yan Shen *et al.*, "Interleukin-6 stimulates Akt and p38 MAPK phosphorylation and fibroblast migration in non-diabetic but not diabetic mice," vol. 12, no. 5, p. e0178232, 2017.
[134] M. R. Duncan and B. J. J. o. I. D. Berman, "Stimulation of collagen and glycosaminoglycan production in cultured human adult dermal fibroblasts by recombinant human interleukin 6," vol. 97, no. 4, pp. 686-692, 1991.
[135] T. Kondo and T. J. I. j. o. l. m. Ohshima, "The dynamics of inflammatory cytokines in the healing process of mouse skin wound: a preliminary study for possible wound age determination," vol. 108, pp. 231-236, 1996.
[136] E. G. Lee, L. R. Luckett-Chastain, K. N. Calhoun, B. Frempah, A. Bastian, and R. M. J. J. o. i. r. Gallucci, "Interleukin 6 function in the skin and isolated keratinocytes is modulated by hyperglycemia," vol. 2019, no. 1, p. 5087847, 2019.
[137] W. D. Short *et al.*, "IL-10 promotes endothelial progenitor cell infiltration and wound healing via STAT3," vol. 36, no. 7, 2022.
[138] B. Latha and M. J. B. Babu, "The involvement of free radicals in burn injury: a review," vol. 27, no. 4, pp. 309-317, 2001.

[139] G. J. B. Arturson, "Pathophysiology of the burn wound and pharmacological treatment. The Rudi Hermans Lecture, 1995," vol. 22, no. 4, pp. 255-274, 1996.

turnitin

Digital Receipt

This receipt acknowledges that Turnitin received your paper. Below you will find the receipt information regarding your submission.

The first page of your submissions is displayed below.

Submission author:	Dr. Muhammad Faraz Bhatti
Assignment title:	Trisk95 Downregulation to Enhance Mitochondrial Function f...
Submission title:	Trisk95 Downregulation to Enhance Mitochondrial Function f...
File name:	MS_thesis_Shumail_Plag.docx
File size:	5.73M
Page count:	44
Word count:	8,592
Character count:	49,325
Submission date:	24-Sep-2024 04:37AM (UTC-0700)
Submission ID:	2463981328

Trisk95 Downregulation to Enhance Mitochondrial Function for Improved Diabetic Wound Healing

Dr. Hussain Mustafab Wahedi
Associate Professor
Dept. of Biomedicine
ASAB - NUST, H-12, Islamabad

Trisk95 Downregulation to Enhance Mitochondrial Function for Improved Diabetic Wound Healing

ORIGINALITY REPORT

16%	12%	10%	3%
SIMILARITY INDEX	INTERNET SOURCES	PUBLICATIONS	STUDENT PAPERS

PRIMARY SOURCES

1	ora.ox.ac.uk Internet Source	1%
2	Iva Bozic, Irena Lavrnja. "Thiamine and benfotiamine: Focus on their therapeutic potential", Heliyon, 2023 Publication	1%
3	www.frontiersin.org Internet Source	1%
4	www.ncbi.nlm.nih.gov Internet Source	1%
5	Swathi Balaji, Emily Steen, Xinyi Wang, Hima V. Vangapandu et al. "IL-10 Promotes Endothelial Progenitor Cell Driven Wound Neovascularization and Enhances Healing via STAT3", Cold Spring Harbor Laboratory, 2019 Publication	<1%
6	www.mdpi.com Internet Source	<1%
7	docslib.org	

	Internet Source	<1 %
8	theses.gla.ac.uk Internet Source	<1 %
9	link.springer.com Internet Source	<1 %
10	Submitted to Universiti Putra Malaysia Student Paper	<1 %
11	d-nb.info Internet Source	<1 %
12	Ayesha Ishtiaq, Attia Bakhtiar, Erica Silas, Javeria Saeed et al. "Pistacia integerrima alleviated Bisphenol A induced toxicity through Ubc13/p53 signalling", Molecular Biology Reports, 2020 Publication	<1 %
13	Submitted to Association of Educators Student Paper	<1 %
14	www.dovepress.com Internet Source	<1 %
15	Submitted to Queen Mary and Westfield College Student Paper	<1 %
16	Wenqian Zhang, Lang Chen, Yuan Xiong, Adriana C. Panayi et al. "Antioxidant Therapy	<1 %

	and Antioxidant-Related Bionanomaterials in Diabetic Wound Healing", Frontiers in Bioengineering and Biotechnology, 2021 Publication	
17	Galdo Bustos, Ulises Ahumada-Castro, Eduardo Silva-Pavez, Andrea Puebla, Alenka Lovy, J. Cesar Cardenas. "The ER-mitochondria Ca2+ signaling in cancer progression: Fueling the monster", Elsevier BV, 2021 Publication	<1 %
18	epub.uni-regensburg.de Internet Source	<1 %
19	Blair Z. Johnson, Andrew W. Stevenson, Cecilia M. Prêle, Mark W. Fear, Fiona M. Wood. "The Role of IL-6 in Skin Fibrosis and Cutaneous Wound Healing", Biomedicines, 2020 Publication	<1 %
20	encyclopedia.pub Internet Source	<1 %
21	www.science.gov Internet Source	<1 %
22	Submitted to Technological University Dublin Student Paper	<1 %
23	Walker D. Short, Emily Steen, Aditya Kaul, Xinyi Wang et al. "IL-10 promotes endothelial	<1 %

progenitor cell infiltration and wound healing via STAT3", The FASEB Journal, 2022
Publication

24	oro.open.ac.uk Internet Source	<1 %
25	Shehla Noor, Sareen Akhtar, Muhammad Farhan Khan, Rahat Abdul Rehman et al. "Preliminary study on mitochondrial DNA analysis from different sports items", Forensic Science International, 2024 Publication	<1 %
26	eprints.soton.ac.uk Internet Source	<1 %
27	storage.googleapis.com Internet Source	<1 %
28	www.genomics.liv.ac.uk Internet Source	<1 %
29	Submitted to Higher Education Commission Pakistan Student Paper	<1 %
30	academic.oup.com Internet Source	<1 %
31	Jing Yang, He Zhao, Shengtao Qu. "Therapeutic potential of fucoidan in central nervous system disorders: A systematic	<1 %

	review", International Journal of Biological Macromolecules, 2024 Publication	
32	Leland J. Cseke, Ara Kirakosyan, Peter B. Kaufman, Margaret V. Westfall. "Handbook of Molecular and Cellular Methods in Biology and Medicine", CRC Press, 2019 Publication	<1 %
33	Weiying Xie, Lili Fang, Shuyuan Gan, Haojun Xuan. "Interleukin-19 alleviates brain injury by anti-inflammatory effects in a mice model of focal cerebral ischemia", Brain Research, 2016 Publication	<1 %
34	Submitted to Bluefield State College Student Paper	<1 %
35	Paul M. Vanhoutte. "Edhf 2002", CRC Press, 2019 Publication	<1 %
36	Submitted to Roosevelt High School Student Paper	<1 %
37	c.coek.info Internet Source	<1 %
38	www.jlr.org Internet Source	<1 %
39	Submitted to University of Greenwich Student Paper	<1 %

40	rbmb.net Internet Source	<1 %
41	repozitorij.pmfst.unist.hr Internet Source	<1 %
42	static.frontiersin.org Internet Source	<1 %
43	Li, Fang, Zheng-Xue Zhang, Yin-Feng Liu, Hui-Qin Xu, Sheng-Tao Hou, and Rong-Yuan Zheng. "2-BFI ameliorates EAE-induced mouse spinal cord damage: Effective therapeutic time window and possible mechanisms", Brain Research, 2012. Publication	<1 %
44	autodocbox.com Internet Source	<1 %
45	dergipark.org.tr Internet Source	<1 %
46	discovery.ucl.ac.uk Internet Source	<1 %
47	ijrm.ssu.ac.ir Internet Source	<1 %
48	www.sid.ir Internet Source	<1 %
49	Submitted to University of Westminster Student Paper	<1 %

50	elib.uni-stuttgart.de Internet Source	<1 %
51	pdffox.com Internet Source	<1 %
52	ruor.uottawa.ca Internet Source	<1 %
53	www.freepatentsonline.com Internet Source	<1 %
54	Parimelazhagan Thangaraj. "Phytomedicine - Research and Development", CRC Press, 2020 Publication	<1 %
55	bmccomplementalternmed.biomedcentral.com Internet Source	<1 %
56	doras.dcu.ie Internet Source	<1 %
57	dr.ntu.edu.sg Internet Source	<1 %
58	etd.lib.metu.edu.tr Internet Source	<1 %
59	kclpure.kcl.ac.uk Internet Source	<1 %
60	oxfordjournals.org Internet Source	<1 %
61	publisher.medfak.ni.ac.rs Internet Source	

		<1 %
62	sro.sussex.ac.uk Internet Source	<1 %
63	wiredspace.wits.ac.za Internet Source	<1 %
64	Dongyou Liu. "Molecular Detection of Human Viral Pathogens", CRC Press, 2019 Publication	<1 %
65	Faisal Almansour, Adib Keikhosravi, Gianluca Pegoraro, Tom Misteli. "Allele-level visualization of transcription and chromatin by high-throughput imaging", Research Square Platform LLC, 2024 Publication	<1 %
66	Gomes, Jéssica Rodrigues. "The Role of a New S. Aureus Hydrolase in Peptidoglycan Degradation", Universidade NOVA de Lisboa (Portugal), 2024 Publication	<1 %
67	Jansen van Rensburg, Gregg. "Biomarker Responses in Three Aquatic Crustacean Species from the Lower Phongolo Floodplain, KwaZulu-Natal, South Africa", University of Johannesburg (South Africa), 2021 Publication	<1 %

68	T. Wang, K. Shankar, M. J. Ronis, H. M. Mehendale. "Mechanisms and Outcomes of Drug- and Toxicant-Induced Liver Toxicity in Diabetes", Critical Reviews in Toxicology, 2008 Publication	<1 %
69	assets-eu.researchsquare.com Internet Source	<1 %
70	discovery.researcher.life Internet Source	<1 %
71	kb.psu.ac.th Internet Source	<1 %
72	orca.cardiff.ac.uk Internet Source	<1 %
73	repository.library.noaa.gov Internet Source	<1 %
74	scholarcommons.usf.edu Internet Source	<1 %
75	www.medrxiv.org Internet Source	<1 %
76	www.researchsquare.com Internet Source	<1 %
77	www2.mdpi.com Internet Source	<1 %

78	Lan-Anh Le, Ross J. Hunter, Victor R. Preedy. "Nanotechnology and Nanomedicine in Diabetes", CRC Press, 2019 Publication	<1 %
79	Shafia, Arina. "Pengaruh Gel Ekstrak Daun Salam (Syzygium Polyanthum) Terhadap Ekspresi Gen Il-10 dan Il-6 Pada Ulkus Traumatikus (Studi Eksperimental in Vivo Pada Tikus Wistar Ulkus Traumatikus)", Universitas Islam Sultan Agung (Indonesia), 2024 Publication	<1 %
80	Nada M. Salah, Heba M. Elbedaiwy, Maged W. Helmy, Noha S. El-Salamouni. "Topical amlodipine-loaded solid lipid nanoparticles for enhanced burn wound healing: A repurposed approach", International Journal of Pharmaceutics, 2024 Publication	<1 %

Exclude quotes	Off	Exclude matches	Off
Exclude bibliography	On		